MedChemNet

World Malaria Day

TOP ARTICLE SUPPLEMENT

CONTENTS

fsg CONNECT

Research Article

For reprint orders, please contact: reprints@futuremedicine.com

Therapeutic Delivery

Antimalarial solid self-emulsifying system for oral use: *in vitro* investigation

Sameer Bhandari[1], Vikas Rana[1] & Ashok K Tiwary[*,1]

[1]Pharmaceutics Division, Department of Pharmaceutical Sciences & Drug Research, Punjabi University, Patiala, Punjab 147 002, India

*Author for correspondence:
Tel.: +91 941 745 7385
aktiwary2@rediffmail.com

Aim: The low aqueous solubility of artemether and lumefantrine makes them less bioavailable. It is expected that by formulating self-microemulsifying drug-delivery systems (SMEDDS), their aqueous solubility and absorption will thus be enhanced. **Results & methodology:** Optimized liquid SMEDDS containing artemether and lumefantrine was adsorbed on Neusilin US2® employing spray drying technique to convert it into solid SMEDDS. Almost 90% of both drugs were released within 15 min in their respective official dissolution media. Drug assay and dissolution rate of solid SMEDDS remained unaltered after 3-month storage at 40°C and 75% relative humidity. **Conclusion:** Reconstitution of solid SMEDDS in water yielded microemulsion with a globule size of 67.74 nm. Complete and faster *in vitro* release of both drugs from solid SMEDDS was observed as compared with that from marketed tablets.

First draft submitted: 16 December 2016; Accepted for publication: 25 January 2017: Published online: 22 February 2017

Keywords: artemether • design of experiment • lumefantrine • Neusilin US2 • solid self-microemulsifying drug-delivery systems • SMEDDS • spray drying

Malaria is a big threat worldwide and is the major cause of death and illness in children and adults, especially in tropical and subtropical countries [1]. Fresh outbreaks are irrevocable due to rapid development activities not keeping pace with cleanliness and hygiene. Moreover, indiscriminate use of existing antimalarials is fostering the spread of resistance by the parasite to monotherapies, which warrants the use of combination therapy for radical cure or force the research scientist to find alternative approaches [2,3]. WHO recommends combination therapy where two or more blood schizontocidal drugs with independent and different mechanism of action are employed against discrete biochemical targets in the parasite. Effectiveness of therapy coupled with rare chance of the mutant parasite to develop resistance to one of the drugs *de novo* during infection is the main reason for combination therapy. WHO recommended various nonartemisinin and artemisinin-based combination therapies, and artemether–lumefantrine combination is one of them [4].

In vitro, artemether and lumefantrine combination has shown to produce better effect against *Plasmodium falciparum* than when used individually [5,6]. *In vivo* data depict that artemether and its major active metabolite dihydroartemisinin rapidly achieve peak plasma concentration in less than 2 h [5–7] and are simultaneously eliminated with an elimination half-life of 1–3 h [5,7,8]. This pharmacokinetic behavior of artemether and dihydroartemisinin decreases parasite load and encourages symptomatic improvement immediately post administration. Lumefantrine, being absorbed and eliminated much slower than artemether, with an elimination half-life of 4–5 days [5,8], eradicates the remaining parasites to prevent recrudescence [7]. These differences in pharmacokinetics of artemether and lumefantrine

FUTURE SCIENCE part of fsg

when used in combination reduce the chances of developing drug resistance in malaria therapy [9].

Artemether is a biopharmaceutics classification system (BCS), Class II drug with low aqueous solubility and high permeability, while lumefantrine exhibits low solubility and permeability (BCS Class IV) [10]. The US FDA label requirement states that artemether–lumefantrine tablets should be taken with meals because the bioavailability of both the drugs is known to be enhanced in the presence of fats. This is well documented in the literature too. Artemether bioavailability is reported to increase twofold and that of lumefantrine to increase 16-fold following administration with high-fat food [7,11]. No dosage form except tablets containing a combination of these drugs is commercially available for human use. It is important to note that the therapeutic potential of artemether and lumefantrine has not been fully exploited due to their low oral bioavailability [11,12] which stems from their poor aqueous solubility and extensive presystemic degradation. Few attempts have been made for enhancing the bioavailability of artemether or lumefantrine by formulating them in various dosage forms like nanoemulsions [13,14], self-microemulsifying drug-delivery systems (SMEDDS) [15–17], self-nanoemulsifying drug-delivery systems [18], solid lipid nanoparticles [19], cyclodextrin complexes [20], liposomes [21] and dry suspension [22]. However, prior art does not reveal any investigation pertaining to formulation containing both the drugs in the form of solid microemulsion preconcentrates. It is logical to expect higher solubility of artemether and lumefantrine in microemulsion formulation. This, in turn, can be hypothesized to enhance their bioavailability and the resultant antimalarial efficacy. In the view of these physiochemical and biopharmaceutical considerations, solid microemulsion preconcentrates containing the combination of artemether and lumefantrine were formulated and optimized with respect to relevant parameter and stability indices.

Materials & methods

Materials

Artemether and lumefantrine were received *ex gratis* from Ipca Laboratories Ltd, Mumbai, India. Labrafil® M 1944 CS (oleoyl macrogol-6 glycerides EP/oleoyl polyoxyl-6 glycerides NF), Peceol™ (glycerol monooleates EP/glycerol monooleates NF) and Labrasol® (caprylocaproyl macrogol-8 glycerides) were obtained as gift samples from Gattefosse, France, supplied by Gattefosse, India. Capmul® MCM (glyceryl mono- and di-caprylo/caprate) was obtained as gift sample from Abitec, USA through Indchem International, Mumbai, India. Solutol HS15 (macrogol 15 hydroxystearate Ph. Eur./polyoxyl 15 hydroxy stearate USP) and Cremophor RH 40 (PEG-35-hydrogenated castor oil) were supplied by BASF India, Ltd through Signet Chemical Corporation Pvt. Ltd, Mumbai, India. Natural oils such as sunflower oil, cottonseed oil, peanut oil and soyabean oil were procured from Kamini oil industries, Mumbai, India, as gift samples. Neusilin UFL2® (magnesium–aluminum metasilicate) manufactured by Fuji Chemical Industry Co., Ltd, Japan was gifted by Gangwal Chemicals Pvt. Ltd, Mumbai, India. Aerosil was received from Smilax Healthcare Pvt. Ltd, Baddi, India. Neusilin US2 was obtained from Sun Pharmaceutical Industries Ltd, Gurgaon, India as a gift sample. Pharmaceutical grade oleic acid, Tween 80, Span 20 and all other chemicals and solvents of analytical grade are manufactured by Loba Chemie, India; canola oil and olive oil were purchased from the local market.

Methods

Analysis of artemether & lumefantrine

Artemether was analyzed using the HPLC method (Supplementary Data 1). Lumefantrine was analyzed by the UV spectrophotometric method (Supplementary Data 2).

Selection of oil, surfactants & cosurfactant

Primarily, different oils were screened for their ability to solubilize maximum quantity of lumefantrine and artemether separately. Oil selected from these studies was mixed with different surfactants (1:1, 1:3 and 3:1) in order to ascertain the capacity of each oil–surfactant mixture (Smix) to solubilize maximum quantity of each drug separately.

The solubility studies for artemether and lumefantrine were carried out by adopting the standard shake flask method of solubility determination. Briefly, an excess amount of artemether or lumefantrine was added to 1 g of oil, oil–Smix and oil–cosurfactant mixture separately in Eppendorf tubes of 1.5 ml capacity. Each Eppendorf tube was vortexed using a cyclomixer for approximately 10 min and then placed in an orbital shaker (Remi, Mumbai, India) at 37 ± 1°C and 150 × *g* r.p.m. for 48 h. Thereafter, the samples were centrifuged at 6000 × g r.p.m. for 20 min (SPINWIN–microcentrifuge, Tarson, India), and aliquots were analyzed spectrophotometrically at a λ_{max} of 264 nm for lumefantrine and by the HPLC method, as discussed earlier for artemether, after suitable dilutions.

Preparation of pseudoternary phase diagrams

The pseudoternary phase diagrams for water, oil, surfactant/Smix were constructed using the water titration method. The ratio of Smix was fixed at 1:1, 1:3 and 3:1 on the basis of weight. For each phase

diagram, nine transparent and homogeneous mixtures of oil:surfactant or oil:Smix at ratios (in w/w) 1:9, 2:8, 3:7, 4:6, 5:5, 6:4, 7:3, 8:2 and 9:1 were prepared by gentle mixing by a magnetic stirrer. These mixtures of oil and surfactant or Smix were carefully titrated with water using a micropipette at a temperature of 30 ± 2°C and visually observed for phase clarity and flowability, and the area under the microemulsion region was calculated using the trapezoidal method.

Preparation of SMEDDS

Based on the solubility study and area of the pseudoternary phase diagrams, the mixture containing selected oil and surfactant/Smix with or without solubilizer and cosurfactant were mixed to form a homogeneous isotropic mixture on a magnetic stirrer at temperature of 30 ± 2°C to form SMEDDS.

Particle size analysis

About 0.1 g of prepared SMEDDS was diluted with 10 ml of double-distilled water prefiltered through 0.45-µm-membrane filters. The average globule size and polydispersity index of the microemulsions were determined by using Malvern Zetasizer Nano S90 (Malvern Instruments, UK). Measurements were carried out at an angle of 90° at 25°C using disposable polystyrene cuvettes. The particle size was measured after 100-times dilution. If required, microemulsions were further diluted with double-distilled filtered water to ensure that the light-scattering intensity was within the instrument's sensitivity range [23].

Design of experiment

On initial screening it was found that concentrations of oil, surfactant/Smix, solubilizer and cosurfactant were important parameters in determining the particle size of SMEDDS. The concentration of oil was fixed at 40% w/w based on the solubilization capacity of the oil for both drugs when added together in SMEDDS. Simplex centroid mixture design was used to statistically optimize the independent variables: concentration of Smix (55–60%), solubilizer (15–25%) and cosurfactant (20–30%) as well as for studying the interaction and quadratic effects of these formulation ingredients on globule size (dependent variable). Different formulations were prepared according to the design points obtained by the design of experiments using Design Expert® software (version 7.0, M/s Stat-Ease, MN, USA). A total of 13 experiments were designed by the software with 12 points on the vertex and 1 center point (in order to allow the estimation of pure error), and experiments were run in random order in triplicates. The average value of the triplicate determination was added to the software.

Preparation of drug-loaded liquid SMEDDS

The optimized formulation suggested by Design of Experiment (DOE) was prepared by dissolving the required amount of artemether and lumefantrine in the optimized mixture of oil, surfactant and cosurfactant at 30°C using a magnetic stirrer (Table 1). This mixture was mixed to obtain a transparent yellowish preparation.

Characterization of drug-loaded liquid SMEDDS

Drug content

Artemether

Drug-loaded liquid SMEDDS containing artemether (2 mg) was weighed in triplicate and mobile phase (2 ml) was added to each test tube to make a solution (1 mg/ml). These solutions were vortexed for 1 min. Analysis was performed by HPLC as detailed earlier.

Lumefantrine

Liquid SMEDDS containing lumefantrine (12 mg) was weighed in triplicate. 0.1 N methanolic HCl (2 ml) was added to each test tube to obtain 6 mg/ml concentration. The microemulsion obtained was further diluted with 0.1 N methanolic HCl to get a final concentration of 10 µg/ml and was analyzed by using the spectrophotometric method for lumefantrine as described earlier.

Self-emulsification studies

The efficiency of self-emulsification of liquid SMEDDS was assessed using USP Dissolution Apparatus II [24]. The optimized liquid SMEDDS (1 ml) was added to water (500 ml) at 37 ± 0.5°C and stirred at 100 × *g* r.p.m. The *in vitro* performance was visually examined using the grading system (Supplementary Data 3).

Percent transmittance studies

Emulsification studies were performed on the optimized liquid SMEDD formulation. Formulation

Table 1. Composition of drug-loaded liquid self-microemulsifying drug-delivery system.

SMEDDS	Ingredient	Quantity (% w/w)†
Drug	Artemether	1.49
	Lumefantrine	8.95
Oil	Oleic acid	35.82
Surfactant	Cremophor RH 40	25.34
	Tween 80	8.42
	Labrasol	8.06
Cosurfactant	Labrafil 1944 CS	11.91

†The quantity of all ingredients in the optimized formulation is less than compared with blank formulation due to the presence of drug in the former formulation.
SMEDDS: Self-microemulsifying drug-delivery system.

(1 ml) was dispersed in water (100 ml) with constant stirring on a magnetic stirrer at 50 × *g* r.p.m. The resulting microemulsion was visually observed for relative turbidity. The microemulsion formed was allowed to stand for 2 h, and its transmittance (%) was measured at 650 nm by a UV spectrophotometer against distilled water as blank [25].

Robustness of dilution/precipitation analysis

The optimized liquid SMEDD formulation was diluted to 250-fold using distilled water or 0.1 N HCl. The diluted microemulsions were observed at 1, 6 and 24 h for any sign of phase separation or drug precipitation and clarity [24].

Thermodynamic stability studies: centrifugation & freeze–thaw test

The optimized liquid formulation was tested for stability by carrying out centrifugation and freeze–thaw tests. The microemulsion formed by dilution of liquid SMEDDS was centrifuged at 3500 × *g* r.p.m. for 30 min. In addition, these microemulsions were subjected to freeze–thaw cycles which included freezing at 4°C and thawing at 45°C for 24 h consecutively for 7 days. The samples were observed visually after centrifugation tests and freeze–thaw cycles.

Cloud point measurement

The cloud point is the temperature above which the formulation clarity turns cloudy in appearance. At higher temperatures, phase separation can occur. The optimized liquid SMEDD formulation was assessed for its stability with respect to phase separation at higher temperature. The formulation was diluted with water in a ratio of 1:100 and placed in a water bath whose temperature was gradually increased. The cloud point was characterized by drop in transmittance measured spectrophotometrically at 650 nm [26].

Preparation of drug-loaded solid SMEDDS

Selection of adsorbent

Oil adsorbing capacity

The optimized liquid SMEDD formulation was diluted with ethanol. Ethanolic solution of liquid SMEDDS (1 g) was mixed with different adsorbents (1 g) dropwise with gentle mixing and heated up to 40°C for evaporating ethanol. Weight of the pure adsorbent (W_a) and that of the adsorbent obtained after ethanol evaporation from the mixture of adsorbent–ethanol solution (W_b) were used for calculating oil adsorbing capacity (OAC). The blend with no significant changes in physical appearance as that of pure adsorbent alone (nongreasy, free flowing and similar texture as that of pure adsorbent) was accepted for W_b. The OAC was estimated using the following formula [27]:

$$OAC = \frac{W_b - W_a}{W_a} \times 100$$

Oil desorbing capacity

Oil desorbing capacity (ODC) was estimated by suspending liquid SMEDDS (1 g) loaded adsorbent (W_b) in water (10 ml) with mild stirring by a magnetic stirrer for 1 h. Then, the suspension was centrifuged at 3000 × *g* r.p.m. for 10 min to recover suspended particles. These were dried and weighed (W_c). The ODC was estimated using the following formula [27]:

$$ODC = \frac{W_b - W_c}{W_c} \times 100$$

Flow properties of Neusilin UFL2 & Neusilin US2

Both Neusilin UFL2 and Neusilin US2 were evaluated for their flow properties before and after the adsorption of liquid SMEDDS by determining the angle of repose, bulk density and tapped density.

Preparation of solid SMEDDS

Neusilin US2 (2.4 g) was suspended in ethanol (250 ml) using a magnetic stirrer, and liquid drug-loaded SMEDDS (5.36 g) was then added. The suspension was spray dried using a lab spray dryer (Model – LU 222, Labultima, Mumbai, India) employing the following conditions: inlet temperature, 35°C; outlet temperature, 35°C; aspiration, 45–50%; and feeding rate, 1 ml/min.

Reconstituted drug-loaded SMEDDS

The prepared blank liquid SMEDDS (1 g), drug-loaded liquid SMEDDS and drug-loaded solid SMEDDS containing liquid SMEDDS (1 g) were dispersed in double-distilled water (10 ml) prefiltered through 0.45-µm-membrane filters by constant stirring with a magnetic stirrer for 60 s.

Characterization of drug-loaded solid SMEDDS

Percentage yield

The percentage yield of spray drying was determined from the weight of adsorbed powder recovered after spray drying (W1) and the total initial weight of starting materials (W2). The formula for calculation of percent yield is as follows:

$$\text{Percentage yeild} = \frac{\text{Weight of spray dried material [W1]}}{(\text{Weight of drug loaded liquid SMEDDS} + \text{Weight of adsorbent [W2]})} \times 100$$

Drug assay

Assay of artemether

Drug-loaded solid SMEDDS containing artemether (2 mg) was weighed in triplicate. Mobile phase (2 ml) was added to each test tube to make a 1 mg/ml concentration.

The suspension was sonicated for 5 min and centrifuged at 6000 × *g* r.p.m. for 10 min. The supernatant was further diluted with the mobile phase to get a final concentration of 50 µg/ml and analyzed according to the HPLC method for artemether.

Assay of lumefantrine

Drug-loaded solid SMEDDS containing lumefantrine (12 mg) was weighed in triplicate. About 2 ml of 0.1 N methanolic HCl was added to each test tube to make 6 mg/ml concentration of suspension. The suspension was sonicated for 5 min and centrifuged at 6000 × *g* r.p.m. for 10 min. The supernatant was further diluted with 0.1 N methanolic HCl to get a final concentration of 10 µg/ml and analyzed according to the spectroscopic method for lumefantrine.

Flow properties of spray dried drug-loaded SMEDDS

Bulk density

Bulk density was determined according to the USP method. The spray dried powder was weighed accurately (W) and was placed into a graduated glass cylinder and leveled carefully without tapping. The apparent volume before tapping was read as Vo, to the nearest graduated unit. The bulk density (untapped density) was calculated in g/ml by the following formula:

$$\text{Bulk Density} = \frac{\text{Weight [W]}}{\text{Untapped volume [Vo]}}$$

Tapped density

The cylinder filled with powder was subjected to 500 tappings and volume was recorded (Va). The tapping was continued till volume difference in two consecutive tapping sets was less than 0.2%. The final volume was recorded as Va and tapped density was determined in g/ml using the following formula:

$$\text{Tapped Density} = \frac{\text{Weight [W]}}{\text{Tapped volume [Va]}}$$

Angle of repose

A glass funnel was placed on a tripod stand, and the powder was placed in the funnel and allowed to flow through the stem of the funnel. The powder was collected as a heap below the funnel with the tip of the stem of funnel just touching the tip of the heap of powder. The radius (r) and height (h) of the heap formed were measured, and the angle of repose was calculated by the following formula:

$$\text{Angle of repose } (\theta) = \tan^{-1}\left(\frac{\text{Height (h)}}{\text{Radius (r)}}\right)$$

Hausner's ratio

Hausner's ratio was calculated by the following formula:

$$\text{Hausner's ratio} = \frac{\text{Tapped density}}{\text{Bulk density}}$$

Carr's index

Carr's index or % compressibility was calculated by the following formula:

$$\text{Carr's index} = 100 \times \left(\frac{\text{Tapped density} - \text{Untapped density}}{\text{Tapped density}}\right)$$

x-ray powder diffraction

To verify the physical state of artemether and lumefantrine in solid SMEDDS, x-ray powder scattering measurements were carried out with an XPert PRO diffractometer (PANalytical, The Netherlands). A voltage of 45 kV and a current of 40 mA for the generator were applied with Cu as the tube anode material. The solids were exposed to Cu Kα radiations, over a range of 10° to 40° of 2θ angles, at an angular speed of 2° (2θ per minute) and a sampling interval of 0.02° [28].

Differential scanning calorimetry

The physical state of artemether and lumefantrine in solid SMEDDS was characterized by differential scanning calorimetric analysis (DSC 131 Evo, Setaram, France). A sample (3–5 mg) was sealed in an aluminum crucible (capacity of 30 µl) with a pin hole in the lid and scanned over the temperature range from 40 to 250°C in an atmosphere of N_2 at a constant heating rate of 10°C per minute.

Scanning electron microscopy

Optimized solid SMEDDS formulation was mounted on the stub and coated with gold particles, and photomicrographs were taken at an accelerating voltage of 10 kV, using SEM 6510 LV (JOEL, Japan).

In vitro drug-release studies

The prepared solid SMEDDS of the optimized formulation was filled in size 000 hard gelatin capsules and subjected to *in vitro* dissolution studies. Release of artemether and lumefantrine from the optimized solid SMEDDS, as well as marketed tablets containing 120 mg lumefantrine and 20 mg artemether, was evaluated using USP XIII Dissolution Testing Apparatus II at 100 rpm in partially degassed water as the dissolution medium for artemether and 0.1 N HCl containing benzalkonium chloride (1% w/v) as well as 0.1 N HCl alone for lumefantrine.

Stability studies

The solid SMEDDS formulation was filled in empty hard gelatin capsules and sealed in HDPE bottles flushed with nitrogen. The samples were subjected to stability studies at 40°C and 75% relative humidity. Samples were kept in a stability chamber (Allyone, Mumbai, India), and analyzed for drug content of artemether and lumefantrine on day 15 and at 1, 2 and 3 months.

Results & discussion

HPLC method: artemether

A retention time of 6.613 ± 0.037 min was observed from the HPLC chromatogram of artemether (Supplementary Data 4). The peaks of different concentrations of artemether revealed an asymmetric factor of 1.47 ± 0.15.

UV method: lumefantrine

UV spectra of lumefantrine exhibited absorbance peaks at 335, 302, 264 and 237 nm. Lumefantrine was quantitated at 264 and 335 nm in accordance with the USP monograph.

Selection of oil, surfactant & cosurfactant

The solubilities of artemether and lumefantrine were determined in various oils. The results revealed that oleic acid solubilizes maximum amount of artemether (428.73 ± 9.3 mg/ml) and lumefantrine (342.73 ± 3.86 mg/ml). Interaction between the carboxyl group of oleic acid and tertiary amine of lumefantrine possibly resulted in higher solubility of lumefantrine in oleic acid [18].

Attempts were made to further augment the solubility of artemether and lumefantine by mixing oleic acid with various hydrophilic surfactants such as Labrasol (HLB-14), Tween 80 (HLB-15), Solutol HS15 (HLB-15), Cremophor RH 40 (HLB-14 to 16) and lipophilic surfactants like Span 20 (HLB-8) and Labrafil M 1944 CS (HLB-4) in three different ratios of 1:3, 1:1 and 3:1 (Table 2).

The results obtained from these experiments were rather discouraging because addition of neither hydrophilic nor lipophillic surfactant was capable of enhancing the solubility of either drug above that observed in oleic acid *per se*. In fact, addition of these surfactants to oleic acid was observed to decrease the solubility of both the drugs with more pronounced effect on lumefantrine's solubility. The very high lipophilicity of lumefantrine could be a major factor for this observation. Furthermore, the solubility of both drugs in oleic acid–hydrophilic surfactant mixtures (Labrasol, Tween 80, Cremophor RH 40 and Solutol HS15) was less as compared with that in the oleic acid–lipophilic surfactant mixtures (Span 20 and Labrafil M 1944 CS). Among lipophilic surfactants, greater solubility of both the drugs in oleic acid in the presence of Labrafil M 1944 CS could be attributed to the property of Labrafil M 1944 CS to attract oils having unsaturated bonds. On the contrary, saturated lipophilic tail of Span 20 cannot be expected to attract oil containing unsaturated bonds [29].

Preparation of pseudoternary phase diagrams

In spite of lipophilic surfactants–oleic acid mixture exhibiting better solubility for both the drugs, it was imperative to evaluate hydrophilic surfactants for their ability to form a o/w microemulsion upon its oral administration. The data obtained from pseudoternary phase diagrams showed that the highest area under the microemulsion region was obtained by using Smix comprising 3:1 ratio of Cremophore RH 40:Tween 80 (Supplementary Data 5).

Influence of oleic acid–Smix ratio on particle size

It was observed that using a mixture of Cremophor RH 40 and Tween 80 in the ratio of 3:1 with oleic acid (6:4) yielded the lowest particle size among the other systems. Further increasing the Smix ratio to 7:3 was not found to aid in decreasing the particle size significantly (Supplementary Data 6).

Influence of adding Labrasol on particle size

It is important to note that the particle size of microemulsion globule was still little above 200 nm. Hence, taking into consideration the area under the microemulsion region exhibited by Labrasol and its easy miscibility with oleic acid, different formulations were prepared by including different proportions of Labrasol in the Smix solution. It is evident from the data that inclusion of 20% Labrasol (OCTL3) yielded the lowest particle size of 168.8 nm (Supplementary Data 7). Further increase in Labrasol concentration did not result in any significant change of particle size. This can be attributed to the fact that gradual increase in concentration of Labrasol led to subsequent decrease in the concentration of Smix.

Influence of adding Labrafil M 1944 CS in Smix on drug precipitation

It is noteworthy that SMEDDS are eventually diluted in gastric fluid on oral administration where they should form microemulsion for exhibiting higher absorption and bioavailability. Hence, the OCTL3 system was prepared by incorporating artemether and lumefantrine and diluted 100-fold with 0.1 N HCl for the evaluation of resultant globule size under simulated gastric conditions. Unfortunately, the process was observed to result in precipitation of lumefantrine. High lipophilicity of lumefantrine ($K_{o/w}$

Table 2. Solubility of artemether and lumefantrine in different oil–surfactant mixtures.

Oleic acid:surfactant	Surfactant	Solubility (mg/ml)	
		Artemether	Lumefantrine
1:3	Labrasol	184.01 ± 1.3	97.00 ± 0.90
	Tween 80	193.79 ± 0.5	99.45 ± 1.54
	Solutol HS 15	194.23 ± 0.8	101.82 ± 0.51
	Cremophor RH 40	188.45 ± 0.7	98.91 ± 0.74
	Span 20	207.64 ± 1.4	91.64 ± 1.03
	Labrafil M 1944 CS	223.58 ± 2.3	109.36 ± 1.16
1:1	Labrasol	246.05 ± 2.5	212.05 ± 6.11
	Tween 80	256.30 ± 2.7	213.18 ± 1.93
	Solutol HS 15	257.99 ± 1.2	223.41 ± 3.54
	Cremophor RH 40	250.08 ± 2.3	210.04 ± 3.03
	Span 20	258.18 ± 1.9	206.59 ± 2.89
	Labrafil M 1944 CS	266.09 ± 1.5	238.86 ± 3.54
3:1	Labrasol	267.63 ± 0.3	286.36 ± 1.93
	Tween 80	275.94 ± 0.3	295.00 ± 5.14
	Solutol HS 15	275.73 ± 3.2	302.27 ± 2.57
	Cremophor RH 40	270.14 ± 1.4	292.08 ± 3.2
	Span 20	282.60 ± 1.0	274.32 ± 4.18
	Labrafil M 1944 CS	303.31 ± 1.1	326. 82 ± 5.14

= 8.34) could be responsible for this phenomenon. Therefore, Labrafil M 1944 CS, which possesses HLB of 4 and had exhibited maximum solubility for lumefantrine (Table 2), was added in different proportions to Smix. Visual observations revealed that inclusion of 20–30% w/w Labrafil M 1944 CS prevented the precipitation of lumefantrine from the microemulsion system.

Design of experiment

From preliminary studies (Supplementary Data 8), concentrations of Smix, Labrasol and Labrafil M 1944 CS were deemed significant in influencing the particle size of liquid SMEDDS. Therefore, concentrations of Smix, Labrasol and Labrafil M 1944 CS were set in the range of, respectively, 55–65%, 15–25% and 20–30% w/w. A simplex centroid mixture design was employed for further investigations. Experiments were carried out in triplicate, and the average value of each experiment was fed in the software. Response data for all experiments are given in Table 3, and the quadratic model showed a superior fit for all the responses (Supplementary Data 9).

3D surface of standard error of design is depicted in Supplementary Data 10. The root mean square error is small and ranges from 0.6 to 0.8 which implies that the error inside the region is nearly uniform.

The design was analyzed for its significance and goodness of fit by analysis of variance (ANOVA) using Design Expert® software version 7.0, M/s Stat-Ease). ANOVA is also helpful in analyzing the effect of different interaction terms on particle size. Since all terms of ANOVA (Supplementary Data 11) were significant, design reduction was not required. F-value compares variation in differences in average responses at designated points using the linear model with the expected experimental variation as estimated from the replicated design point. The model F-value of 46.3347 implied that the model was significant. The p-value represents the probability of achieving the F-value. p-values of model and linear terms less than 0.05 proved significance of the model. The model was also evaluated for lack of fit. The p-value of 0.0732 for lack of fit implied that lack of fit was insignificant and the model fitted well. The final obtained model to predict particle size is given in Equation (1) in pseudo terms:

Particle size = + 89.6535A + 92.4468B + 177.1501C + 75.0372AB - 151.903AC - 139.743BC

where A, B and C represent fraction of Smix, Labrasol and Labrafil M 1944 CS, respectively.

The particle size predicted by the model was similar to the actual particle size obtained experimentally (Supplementary Data 12). A close confirmation is obtained in all cases as all the points fall close to the

trend line where an R^2 value of 0.9707 was obtained. The model had an adjusted R^2 value of 0.9497 and a predicted R^2 value of 0.8504. A close conformance of adjusted and predicted R^2 values made it evident that the model was able to predict the response adequately. Signal-to-noise ratio measured by adequate precision was 18.205 which is pretty high to imply the adequacy of model used to navigate design space. 3D surface plots of model graph representing the effect of Smix, Labrasol and Labrafil M 1944 CS on the particle size are depicted in Supplementary Data 13.

Effect of components

In a mixture type of design, the constants for variables A, B and C give the value for response at the vertex, in other words, when that component is at the maximum level. When the value of A is 1, B and C would be 0, and the value of rest of the components would be equivalent to 0.

The interaction term describes the effect of response in the design space in a better way. As observed from ANOVA (Supplementary Data 11), the F-values for AC and BC are distinctly greater than AB. Moreover, the smaller magnitude of 'p' for F-values of AC and BC than AB confirmed stronger effect of AC and BC on particle size. Since the value of the constants for AC and BC is negative, it can be inferred that these interactions provided a positive effect on decreasing particle size.

Diagnostics

All points of normal plot of residuals (Supplementary Data 14) follow a straight line indicating that residuals followed a normal distribution. Furthermore, the Box-Cox plot (Supplementary Data 15) also affirmed that the model had predicted the response well and further transformation was unnecessary.

Optimization

The main objective of the study was to determine the composition of surfactant system which would promote formation of small particles. As observed in Figure 1, particle size reaches a minimum at a certain fraction of components. By setting factor goals within range and response goals to minimum numerical, optimization was carried out to obtain a set of values for all factors. 3D surface plot of desirability is depicted in Figure 1.

Summary of design of experiment

The 3D surface plot for particle size depicts the existence of least particle size in the design space. The optimized system having a composition of 62.88% Smix, 15% Labrasol and 22.12% Labrafil M 1944 CS was capable of yielding a particle size of 82.83 nm. The experimental value for the particle size for the given set of conditions was 88.53 nm which was in close confirmation of the predicted value (Supplementary Data 16).

Characterization of drug-loaded liquid SMEDDS

Drug content

The drug content of artemether and lumefantrine in optimized liquid SMEDDS was found to be in the range of 98.43–100.65% and 99.24–100.32%, respectively, indicating uniform dispersion of drug in the formulation.

Table 3. Response data for mixture study.

Run	Factor A percentage Smix (%)	Factor B percentage Labrasol	Factor C percentage Labrafil M 1944 CS (%)	Response particle size (nm)
1	55.000	20.000	25.000	103.200
2	55.000	15.000	30.000	176.500
3	65.000	15.000	20.000	86.710
4	65.000	15.000	20.000	94.980
5	55.000	25.000	20.000	92.030
6	56.667	21.667	21.667	88.530
7	55.000	25.000	20.000	93.010
8	56.667	16.667	26.667	116.310
9	60.000	20.000	20.000	116.830
10	61.667	16.667	21.667	79.410
11	55.000	15.000	30.000	176.500
12	60.000	15.000	25.000	101.000
13	58.333	18.333	23.333	99.370

Smix: Surfactant mixture.

Particle size

It is interesting to note that the average particle size of optimized liquid SMEDD formulation was reduced from 88.53 nm (blank formulation) to 61.01 nm (after drug loading) (Supplementary Data 17). This unexpected observation is in consonance with the reports of decrease in particle size from 120 to 37.96 nm of lumefantrine-loaded oleic acid self-nanoemulsifying drug-delivery system formulation [18]. This fourfold reduction in particle size was proposed to be due to the possibility of lumefantrine–oleic acid complex promoting its own 'self-emulsification.' The interaction between the carboxylic acid group of oleic acid and the amine group of lumefantrine to form an ion pair was confirmed with the help of ζ potential measurements of plain oleic acid nanoemulsion (-6.73 mV) and lumefantrine-loaded oleic acid nanoemulsion (+4.4 mV), which resulted in higher solubility of lumefantrine in oleic acid [18].

Similar ionic interactions between lumefantrine and oleic acid can be expected to have occurred in the presently optimized SMEDD formulation. In addition, this highly lipophilic molecule (lumefantrine) might have occupied the core of oleic acid, which would have attracted the lipophilic chain of the surfactant toward itself, which would restrict the mobility of surfacant molecules, thus reducing the size of the oil globule [30]. Also, the role of undissolved drug deposited at the surface of emulsion globules, thereby restricting the mobility of the surfactant molecules resulting in the decrease in the particle size, cannot be ruled out.

Self-emulsification & stability studies

The results of self-emulsification and precipitation studies revealed a short time of 10 s for emulsification providing a clear yellowish microemulsion with a transmittance of 86.39 ± 3.18%, which showed no sign of phase separation or drug precipitation in an optimized liquid SMEDDS formulation indicating stability of the prepared liquid SMEDDS after dilution. Furthermore, the thermodynamic stability was established by repeated centrifugation or freeze–thaw cycles. Moreover, the observed high cloud point of 79°C indicated its stability and resistance toward phase separation and reduction of drug solubility.

Preparation of solid SMEDDS

OAC & ODC

The results of OAC and ODC of Neusilin UFL2, Neusilin US2 and Aerosil 200 Pharma clearly established the superiority of Neusilin grades over Aerosil 200 Pharma in adsorption as well as desorption (Supplementary Data 18).

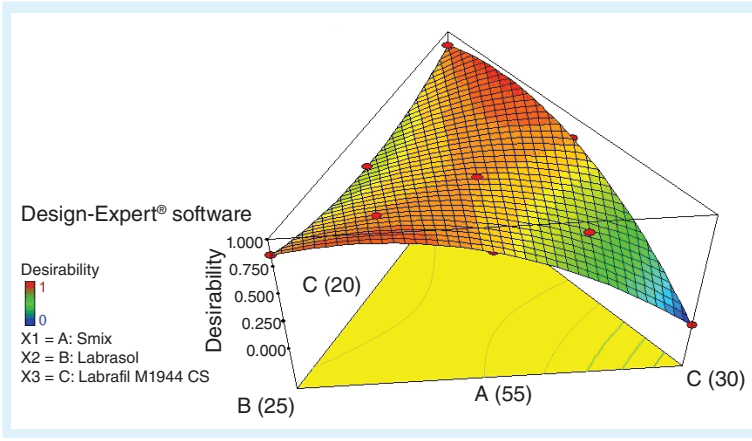

Figure 1. 3D graph of desirability of particle size.
Smix: Surfactant mixture.

Flow properties of Neusilin UFL2 & Neusilin US2

Since the oil adsorption and oil desorption capacities of Neusilin UFL2 and Neusilin US2 were similar and superior to Aerosil 200 Pharma, both Neusilin UFL2 and Neusilin US2 were further evaluated for their flow properties. Based on the morphology and flow properties, Neusilin US2 was selected for spray drying as it depicted better flow as compared with Neusilin UFL2 (Supplementary Data 19).

Characterization of solid SMEDDS

The spray dried product recovered from the cyclones of a spray dryer provided a yield of 66.39 ± 1.73%. A comparison of data (Supplementary Data 19) revealed good flow and compressibility of solid SMEDDS prepared from Neusilin US2. The assay in optimized solid SMEDDS was found to be 95.87 ± 1.37% and 97.69 ± 2.13% for artemether and lumefantrine, respectively, indicating uniform dispersion of drug in the formulation. Upon reconstitution, the adsorbed drug-loaded liquid SMEDDS desorbed from the surface of Neusilin US2, leading to the formation of microemulsion with a globule size and polydispersity index of, respectively, 67.74 nm and 0.408, indicating the presence of segregated globules in a narrow size range (Supplementary Data 20).

x-ray powder diffraction

x-ray diffraction patterns of artemether (Figure 2A) and lumefantrine (Figure 2B) were sharp, thus indicating their crystalline character. Neusilin US2 appeared to be amorphous in nature (Figure 2C). The diffractogram of physical mixture containing Neusilin US2 and both drugs (Figure 2D) exhibited characteristics of both drugs. However, peak representatives of such a crystalline character of both drugs were not observed in the diffractogram of solid SMEDDS (Figure 2E). This could be due to the presence of both

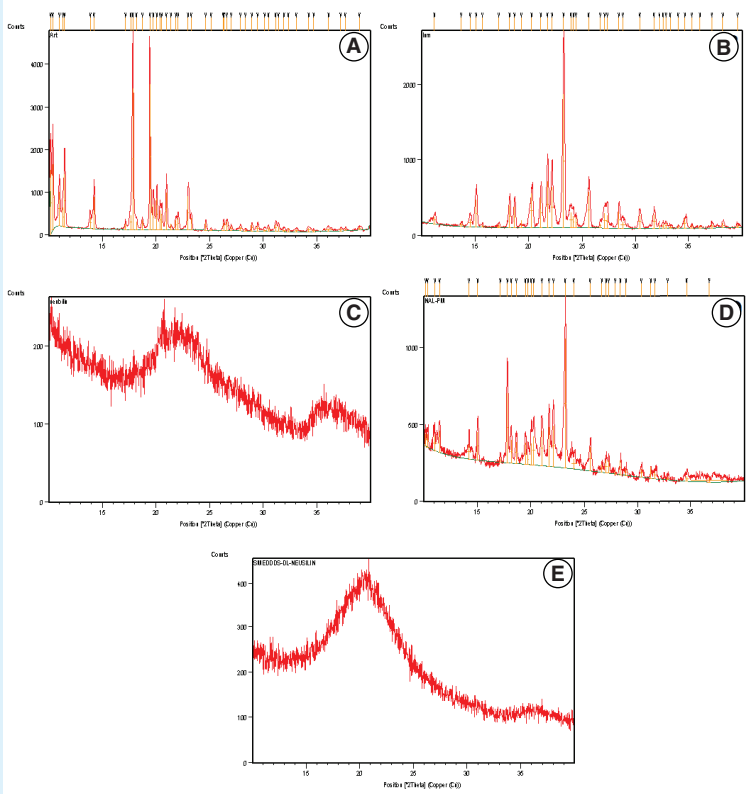

Figure 2. x-ray powder diffractogram. (A) Artemether; **(B)** lumefantrine; **(C)** Neusilin US2; **(D)** physical mixture containing Neusilin US2, artemether and lumefantrine; and **(E)** drug-loaded solid SMEDDS.
SMEDDS: Self-microemulsifying drug-delivery system.

drugs in oil solubilized form that was subsequently adsorbed on Neusilin US2 [28].

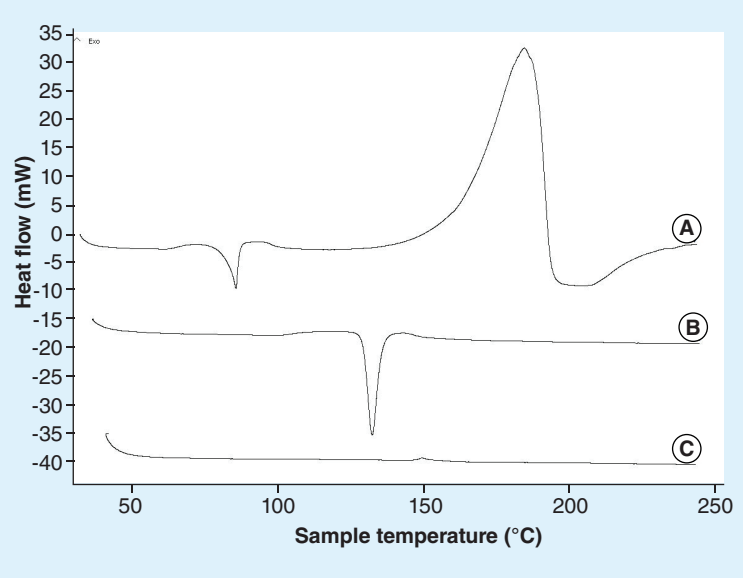

Figure 3. Differential scanning calorimetric profiles. (A) Artemether, **(B)** lumefantrine and **(C)** drug-loaded solid SMEDDS.
SMEDDS: Self-microemulsifying drug-delivery system.

Differential scanning calorimetry

Artemether (Figure 3A) and lumefantrine (Figure 3B) exhibited sharp endotherms at peak temperature of, respectively, 86.57 and 133.09°C, which are their melting points. These characteristic endothermic transitions were absent in thermograph of solid SMEDDS (Figure 3C). This could be ascribed to the presence of both drugs in oil solubilized form in solid SMEDDS and corroborates with the results of x-ray diffraction studies. In addition, the role of surfactants in preventing crystallization of drugs cannot be ruled out [28].

Scanning electron microscopy

The scanning electron micrographs of plain Neusilin US2 at 2200× magnification is shown in Figure 4A. It is clearly evident from Figure 4A that Neusilin US2 is a highly porous and granular material with relatively large pores, whereas liquid SMEDDS after spray drying (Figure 4B) can be seen to have covered most of the pores and also appeared to have been partially spread on the surface of Neusilin US2 particles.

In vitro dissolution studies

From *in vitro* dissolution studies, it was revealed that artemether was slowly released from marketed tablets in water (USP official media), whereas, approximately all artemethers were released in water within 15 min from the optimized solid SMEDD formulation (Figure 5A).

The release of lumefantrine from marketed formulation in 0.1N HCl was negligible. Addition of benzalkonium chloride (1% w/v) to 0.1 N HCl (USP official media) was able to promote the release of lumefantrine to the extent of approximately 80% in 1 h. The fastest release of lumefantrine in 0.1 N HCl was observed in solid SMEDDS where approximately 90% release was obtained in 15 min (Figure 5B).

Stability studies

The optimized solid SMEDDS formulation was packed in hard gelatin capsule shells (000 size) and sealed in HDPE bottles flushed with nitrogen. No significant change was observed in the drug content and drug release of artemether and lumefantrine from solid SMEDDS after 3 months of storage at 40°C and 75% relative humidity in the stability chamber. The formulation was compatible with hard gelatin capsule shells as no sign of deformation of capsule shells was observed. Also, no significant changes were observed in the appearance and microemulsifying property. Thus, stability studies established the stability of the developed optimized formulation and its compatibility with hard gelatin capsules.

Conclusion

Artemether and lumefantrine possess low aqueous solubility due to their high lipophilicity and hence exhibit low oral bioavailability. Central composite design of experiment was successfully employed to prepare microemulsion preconcentrates using 62.88, 15 and 22.12% of Smix, Labrasol and Labrafil M 1944 CS, respectively, as surfactant phase. The oil:surfactant ratio was 4:6. The optimized liquid SMEDD formulation possessed a particle size of 88.53 nm which was in close agreement with the particle size predicted by design of experiments. Microemulsion preconcentrate (2 g) was adsorbed on Neusilin US2 (1 g) to yield a free-flowing powder. This formulation was observed to yield a particle size of 67.74 nm on dilution with water. High solubility of artemether (428.73 mg) and lumefantrine (342.73 mg) coupled with small particle size and rapid release from SMEDDS in water as well as 0.1 N HCl with respect to marketed tablet suggests high potential of solid SMEDDS for further evaluation in enhancing their bioavailability and efficacy of antimalarial activity.

Future perspective

The highly lipophilic nature of lumefantrine (BCS Class IV) and artemether (BCS Class II) makes them less soluble and bioavailable. Their combination is recommended by WHO as a combination therapy for early treatment and preventing drug resistance and recrudescence of malaria. Formulating this drug combination in a microemulsion form is a facile method for enhancing their solubility and bioavailability. However, due to the high content of oil (~40% v/v), liquid SMEDDS are required to be converted to solid SMEDDS. These systems are easy to formulate and scale up as well as exhibit significant improvement in handling, transportation and patient compliance.

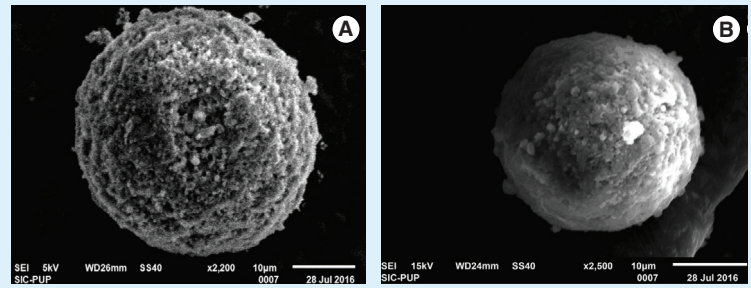

Figure 4. Scanning electron photomicrographs. (A) Neusilin US2 at 2200× and **(B)** spray dried liquid SMEDDS on Neusilin US2 at 2500×.
SMEDDS: Self-microemulsifying drug-delivery system.

The spray drying method was successfully employed to produce a free-flowing powder formulation containing liquid SMEDDS adsorbed on Neusilin US2. The rate of spray and temperature of drying influenced the properties of the resultant dry powder. Furthermore, adsorption as well as desorption of oil containing solubilized drugs and globule size of desorbed oil needed special attention. The former dictates the requirement of powder quantity per dose whereas the later reflects efficiency of drug release.

Despite satisfactory *in vitro* results of optimized solid SMEDDS, it seems to be essential to investigate other novel adsorbents for increasing the drug loading, which would, in turn, decrease the quantity of solid SMEDDS per dose. It would be interesting to evaluate the compaction behavior of solid SMEDDS powder, which may necessitate use of special excipients due to the high oil content in solid SMEDDS. Eventually, the *in vivo* performance of the optimized

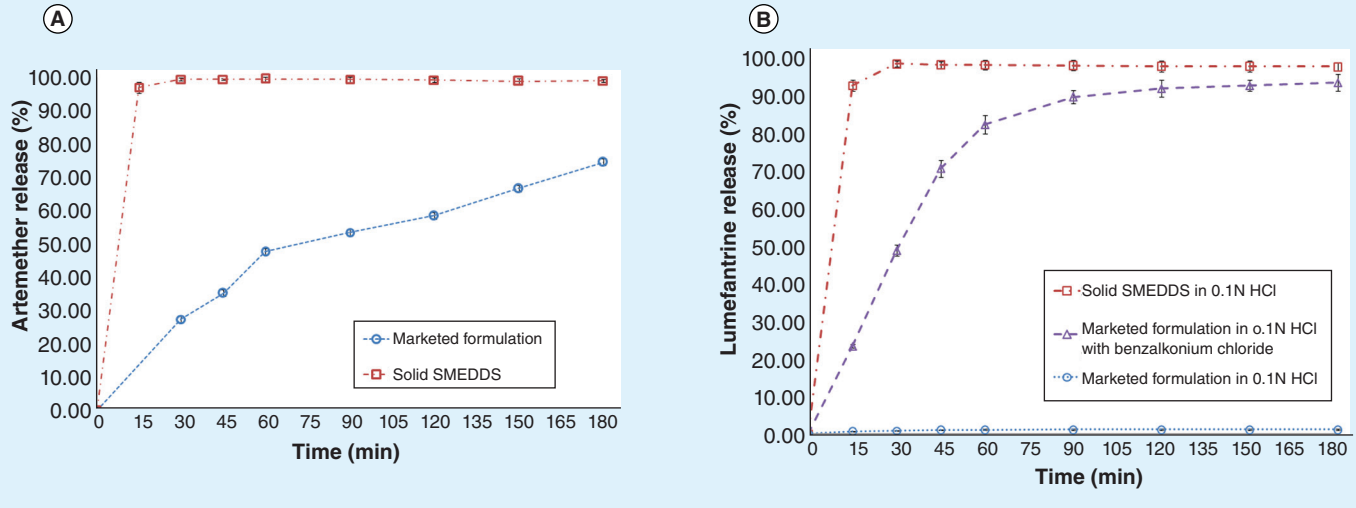

Figure 5. *In vitro* release profiles. (A) Artemether in partially degassed water and **(B)** lumefantrine in 0.1 N HCl as well as 0.1 N HCl containing benzalkonium chloride (1% w/v).

formulation is needed to be evaluated for pharmacokinetics and treatment of malaria in the experimental model before advocating its use in human beings.

Financial & competing interests disclosure

The authors would like to acknowledge the financial assistance provided by University Grants Commission, Government of India, New Delhi, India under major research project (Grant No. 41–711/2012(SR). The scholarship provided by University Grants Commission, Government of India, New Delhi, India, vide letter no. F.4.25–1/2013–14(BSR)/7–265/2009/(BSR) is also acknowledged. The authors have no other relevant affiliations or financial involvement with any organization or entity with a financial interest in or financial conflict with the subject matter or materials discussed in the manuscript. This includes employment, consultancies, honoraria, stock ownership or options, expert testimony, grants or patents received or pending, or royalties.

No writing assistance was utilized in the production of this manuscript.

Ethical conduct of research

The authors state that they have obtained appropriate institutional review board approval or have followed the principles outlined in the Declaration of Helsinki for all human or animal experimental investigations. In addition, for investigations involving human subjects, informed consent has been obtained from the participants involved.

Executive summary

- Simplex centroid design was successfully employed to optimize self-microemulsifying drug-delivery system (SMEDD) formulation containing artemether and lumefantrine followed by its conversion to solid SMEDD by adsorption on Neuslin US2 using the spray drying method.
- Each 5 g of the free flowing optimized formulation contained 1 g of lumefantrine and 0.17 g of artemether, and yielded a globule size of 67.74 nm on dispersing in water.
- The release of lumefantrine in 0.1 N HCl and artemether in water, respectively, was 92.86 and 96.94% in 15 min from the optimized solid SMEDD formulation. On the other hand, marketed formulation exhibited negligible release of both drugs in respective media in 15 min. Even in the presence of benzalkonium chloride (1% w/v), the marketed formulation released only 23.36% of lumefantrine in 15 min.
- The optimized solid SMEDD formulation holds great promise for evaluation of its pharmacokinetic and antimalarial efficacy.

References

1 Carballeira NM. New advances in fatty acids as antimalarial, antimycobacterial and antifungal agents. *Prog. Lipid Res.* 47(1), 50–61 (2008).

2 Fischer PR, Bialek R. Prevention of malaria in children. *Clin. Infect. Dis.* 34(4), 493–498 (2002).

3 Snow RW, Trape JF, Marsh K. The past, present and future of childhood malaria mortality in Africa. *Trends Parasitol.* 17(12), 593–597 (2001).

4 WHO, Guidelines for the treatment of malaria. http://apps.who.int/iris/bitstream/10665/162441/1/9789241549127_eng.pdf?ua=1&ua=1

5 Premji ZG. Coartem®: the journey to the clinic. *Malar. J.* 8(Suppl. 1), S3 (2009).

6 Hassan AM, Bjorkman A, Wernsdorfer WH. Synergism of benflumetol and artemether in *Plasmodium falciparum*. *Am. J. Trop. Med. Hyg.* 61(3), 439–445 (1999).

7 White NJ, vanVugt M, Ezzet F. Clinical pharmacokinetics and pharmacodynamics and pharmacodynamics of artemether–lumefantrine. *Clin. Pharmacokinet.* 37(2), 105–125 (1999).

8 Kowaro G, Mwai L, Nzila A. Artemether/lumefantrine in the treatment of uncomplicated falciparum malaria. *Expert Opin. Pharmacother.* 8(1), 75–94 (2007).

9 White NJ. Preventing antimalarial drug resistance through combinations. *Drug Resist. Updat.* 1(1), 3–9 (1998).

10 Lindenberg M, Kopp S, Dressman JB. Classification of orally administered drugs on the World Health Organization model list of essential medicines according to the biopharmaceutics classification system. *Eur. J. Pharm. Biopharm.* 58(2), 265–278 (2004).

11 Ashley EA, Stepniewska K, Lindegardh N *et al.* How much fat is necessary to optimize lumefantrine oral bioavailability? *Trop. Med. Int. Health.* 12(2), 195–200 (2007).

12 Karbwang J, Na-Bangchang K, Congpuong K, Molunto P, Thanavibul A. Pharmacokinetics and bioavailability of oral and intramuscular artemether. *Eur. J. Clin. Pharmacol.* 52(4), 307–310 (1997).

13 Joshi M, Pathak S, Sharma S, Patravale V. Design and *in vivo* pharmacodynamics evaluation of nanostructured lipid carriers for parenteral delivery of artemether: Nanoject. *Int. J. Pharm.* 364(1), 119–126 (2008).

14 Laxmi M, Bhardwaj A, Mehta S, Mehta A. Development and characterization of nanoemulsion as carrier for the enhancement of bioavailability of artemether. *Artif. Cells Nanomed. Biotechnol.* 43(5), 334–344 (2015).

15 Joshi M, Pathak S, Sharma S, Patravale V. Solid microemulsion preconcentrate (NanOsorb) of artemether for effective treatment of malaria. *Int. J. Pharm.* 362(1–2), 172–178 (2008).

16 Mandawgade SD, Sharma S, Pathak S, Patravale V. Development of SMEDDS using natural lipophile: application to β-artemether delivery. *Int. J. Pharm.* 362(1–2), 179–183 (2008).

17 Patil S, Suryavanshi S, Pathak S, Sharma S, Patravale V. Evaluation of novel lipid based formulation of β-artemether and lumefantrine in murine malaria model. *Int. J. Pharm.* 455(1–2), 229–234 (2013).

18 Patel K, Sarma V, Vavia P. Design and evaluation of lumefantrine–oleic acid self nanoemulsifying ionic complex for enhanced dissolution. *Daru* 21(1), 27–36 (2013).

19 Raina N, Goyal AK, Pillai CR, Rath G. Development and characterization of artemether loaded solid lipid nanoparticles. *Ind. J. Pharm. Edu. Res.* 47(2), 123–128 (2013).

20 Yang B, Lin J, Chen Y, Liu Y. Artemther/hydroxypropyl-β-cyclodextrin host–guest system: characterization, phase-solubility and inclusion mode. *Bioorg. Med. Chem.* 17, 6311–6317 (2009).

21 Chimanuka B, Gabriels M, Detaevernier MR, Plaizier-Vercammen JA. Preparation of β-artemether liposomes, their HPLC-UV evaluation and relevance for clearing recrudescent parasitaemia in *Plasmodium chabaudi* malaria-infected mice. *J. Pharm. Biomed. Anal.* 28(1), 13–22 (2002).

22 Atemnkeng MA, Marchand E, Plaizier-Vercammen J. Assay of artemether, methylparaben and propylparaben in a formulated paediatric antimalarial dry suspension. *J. Pharm. Biomed. Anal.* 43(2), 727–732 (2007).

23 Attwood D. Microemulsions. In: *Colloidal Drug-Delivery Systems*. Kreuter J (Ed.). Marcel Dekker, NY, USA, 31–71 (1993).

24 Singh AK, Chaurasiya A, Singh M, Upadhyay SC, Mukherjee R, Khar RK. Exemestane loaded self-microemulsifying drug-delivery system (SMEDDS): development and optimization. *AAPS PharmSciTech.* 9(2), 628–634 (2008).

25 Date AA, Nagarsenker MS. Design and evaluation of self-nanoemulsifying drug-delivery systems (SNEDDS) for Cefpodoxime Proxetil. *Int. J. Pharm.* 329(1–2), 66–72 (2007).

26 Zhang P, Liu Y, Feng N, Xu J. Preparation and evaluation of self-microemulsifying drug-delivery system of oridonin. *Int. J. Pharm.* 355(1–2), 269–276 (2008).

27 Singh K, Tiwary AK, Rana V. Ethylenediaminediacetic acid bis(carbido amide chitosan): synthesis and evaluation as solid carrier to fabricate nanoemulsion. *Carbohydr. Polym.* 95(1), 303–314 (2013).

28 Yi T, Wan J, Xu H, Yang X. A new solid self-microemulsifying formulation prepared by spray-drying to improve the oral bioavailability of poorly water soluble drugs. *Eur. Pharm. Biopharm.* 70(2), 439–444 (2008).

29 Griffin WC. Calculation of HLB values of nonionic surfactants. *J. Soc. Cosmet. Chem.* 5, 249–256 (1954).

30 Park KM, Kim CK. Preparation and evaluation of flurbiprofen loaded microemulsion for parenteral delivery. *Int. J. Pharm.* 181(2), 173–179 (1999).

Review

For reprint orders, please contact reprints@future-science.com

Future Medicinal Chemistry

Spiroindolone NITD609 is a novel antimalarial drug that targets the P-type ATPase PfATP4

Helen Turner
Department of Life, Health & Chemical Sciences, The Open University, Walton Hall, Milton Keynes, MK7 6AA, UK
hels_turner@yahoo.co.uk

Malaria is caused by the *Plasmodium* parasite and is a major health problem leading to many deaths worldwide. Lack of a vaccine and increasing drug resistance highlights the need for new antimalarial drugs with novel targets. Antiplasmodial activity of spiroindolones was discovered through whole-cell, phenotypic screening methods. Optimization of the lead spiroindolone improved both potency and pharmacokinetic properties leading to drug candidate NITD609 which has produced encouraging results in clinical trials. Spiroindolones inhibit PfATP4, a P-type Na^+-ATPase in the plasma membrane of the parasite, causing a fatal disruption of its sodium homeostasis. Other diverse compounds from the Malaria Box appear to target PfATP4 warranting further research into its structure and binding with NITD609 and other potential antimalarial drugs.

First draft submitted: 28 August 2015; Accepted for publication: 16 November 2015; Published online: 29 January 2016

Keywords: cipargamin • KAE609 • malaria • NIDT609 • PfATP4 • *Plasmodium* • spiroindolone

Introduction/background

Malaria is an infectious disease caused by the malaria parasite *Plasmodium* and transmitted by female *Anopheles* mosquitoes. The four main species that infect humans are *Plasmodium falciparum, Plasmodium vivax, Plasmodium ovale* and *Plasmodium malariae. P. falciparum* and *P. vivax* are the most common with *P. falciparum* causing the most deaths globally [1]. WHO estimates there were 198 million cases of malaria and 584,000 malaria deaths in 2013 [2], which is a great improvement since 20 years previous when it caused over 1 million deaths per year [3].

The life cycle of the malaria parasite is complex with several life stages involving both mosquito and human hosts (Figure 1).

Currently, there is no vaccine licensed for use against malaria, however, it is hoped a vaccination that offers some protection will soon be introduced. Most existing antimalarial drugs act against the asexual blood stages of the parasite. Primaquine is the only drug approved that acts against the dormant liver stages of *P. vivax* whose reactivation lead to relapse [4]. For many years chloroquine and sulphadoxine–pyrimethamine were the principal antimalarial treatments; however, resistance to both drugs led to increased morbidity and mortality from malaria. Artemisinin-based combination therapies (ACTs), which contain a combination of an artemisinin derivative and another antimalarial drug with a different mechanism of action, are recommended to reduce the risk of drug resistance [1]. ACTs are a major factor in the increased malaria control, consequently it is of great concern that *P. falciparum* has developed some resistance to artemisinin derivatives in south-east Asia [5].

Increasing resistance of *Plasmodium* to the existing malaria treatments including artemisinin and its derivatives [5], highlight the need for new antimalarial drug therapies. Key factors in considering the target product profile (TPP)

FUTURE SCIENCE part of fsg

include the vulnerability of many of the patients (many of whom are young children and pregnant women), the lack of medical supervision under which drugs are administered and the need for patient compliance.

Ideally new antimalarial drugs should [1,6]:

- Be effective against the blood stages of the key species of parasite that cause malaria in humans, including those with drug resistance;
- Kill the hypnozoites of *P. vivax* and *P. ovale* therefore preventing relapse;
- Kill the gametocytes to prevent transmission;
- Kill sporozoites and exo-erythrocytic schizonts therefore preventing the initial infection when used prophylactically;
- Have a novel mechanism of action;
- Have good oral availability;
- Be safe;
- Cure by a single dose;
- Be cheap to produce.

Discovery of spiroindolones as antimalarial agents

At a time when there was optimism that the rational drug design approach, based on the molecular understanding of the biology of the malaria parasite, would produce new antimalarial drugs, the spiroindolones (spirotetrahydro β-carbolines: synthetic compounds with two stereocenters consisting of a β-carboline structure connected through a centralspiroatom to an indole structure) were identified using older, whole-cell, phenotypic screening methods based on the growth inhibition of *P. falciparum* [7]. A library of

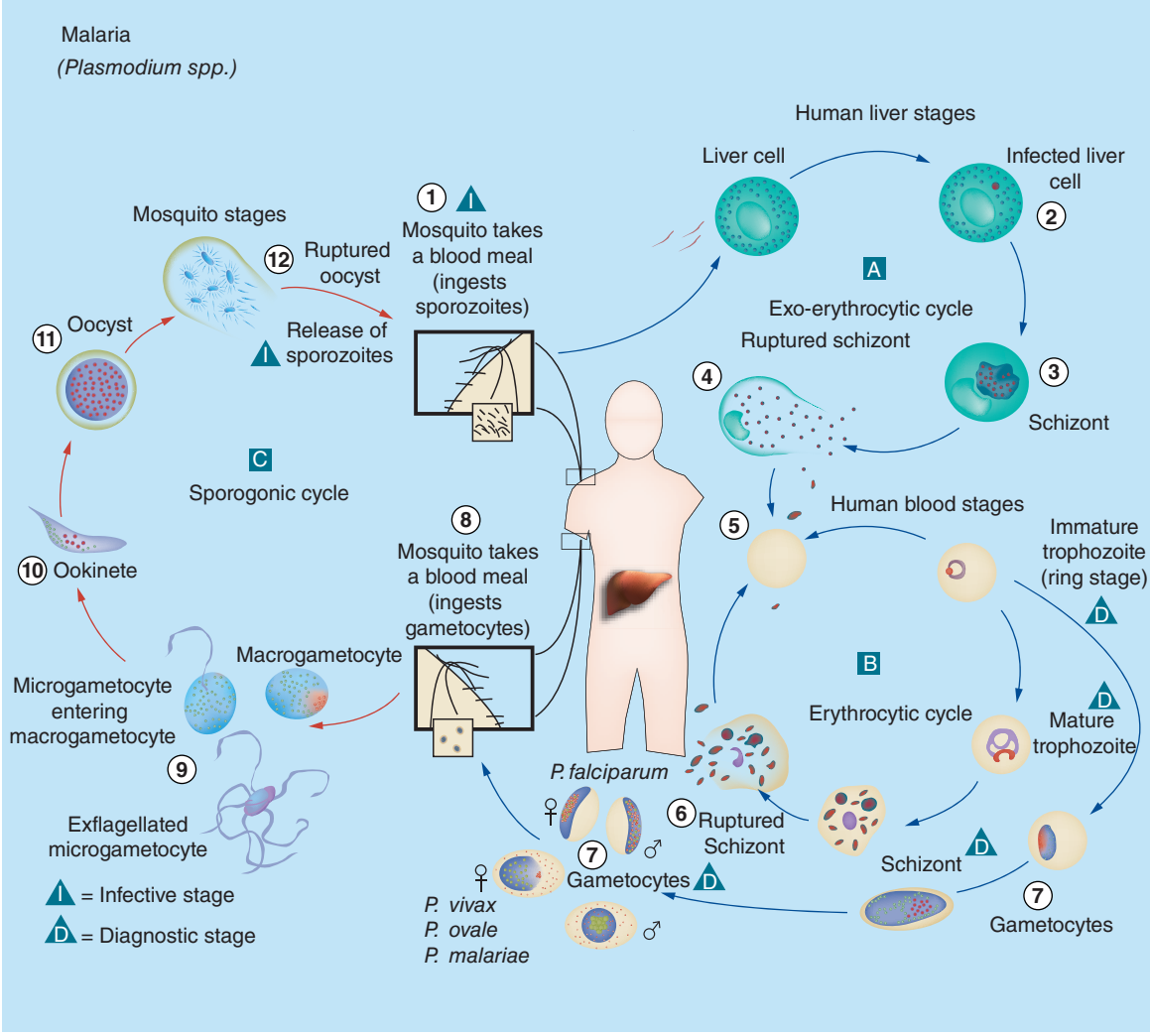

Figure 1. Malaria parasite life cycle. The life cycle is complex involving both human and mosquito hosts. Reproduced from Public Health Image Library, Centers for Disease Control and Prevention [10].

12,000 pure natural and structurally similar synthetic molecules was screened using whole-cell proliferation assays with cultured cells from intra-erythrocytic *Plasmodium* parasites [8,9]. The screening found 275 compounds with submicromolar activity against *P. falciparum*. This was reduced to 17 compounds by excluding those that lacked activity against multidrug-resistant forms of the parasite and any showing cytotoxicity to mammalian cells. Since it is important that a new antimalarial drug can be administered in tablet form the oral bioavailability of the remaining compounds was assessed. Based on its activity against *Plasmodium* and favorable pharmacokinetic profile a synthetic compound (**1**) related to the spiroazepineindole class was selected for medicinal chemistry lead optimization. Compound **1** was found to possess good oral bioavailability in mice with F = 59% and an oral half-life of nearly 4 h [4].

The initial compound identified (**1**) was a racemic mixture consisting of 1R,3S & 1S,3R and 1S,3S & 1R,3R pairs of enantiomers, which were found to have moderate potency against wild-type (NF54) and chloroquine-resistant (K1) strains of *Plasmodium* (Figure 2). A single 100 mg/kg dose of racemic compound **1** was found to lead to a 96% decrease in parasitemia in the *P. berghei*-infected mouse model.

The reaction to create compound **1** yielded an unequal mixture such that there was a 9:1 excess of the 1R,3S & 1S,3R pair of enantiomers [9]. Structure–activity relationship (SAR) analysis showed that the 1R,3S stereoisomer (**1a**) was over 250-times more potent against *P. falciparum* than the 1S,3R stereoisomer (**1b**) (Figure 2). Structure–activity relationship analysis of further spiroindolone compounds consistently indicated that the 1R,3S stereoisomer was essential to be active against *P. falciparum* [9]. Only one enantiomer being active suggested the existence of a discreet target.

Optimization of spiroindolone lead led to drug candidate NITD609

Most antimalarial drugs act on the parasite in the blood stages therefore it is desirable for the drug to stay in the plasma compartment and not to enter the body fat. With this in mind, Yeung *et al.* made substitutions to the bromine atom on compound 1 to make the molecule less lipophilic, since lipophilic molecules are more likely to enter the adipose tissue from the plasma. Replacing the 5′-bromide with a 5′-chloro was found to produce a compound with improved balance of potency, pharmacokinetics and synthetic accessibility [9] (Figure 3 – Compound **2**). However, mono- and disubstitutions with other halogens produced unfavorable results.

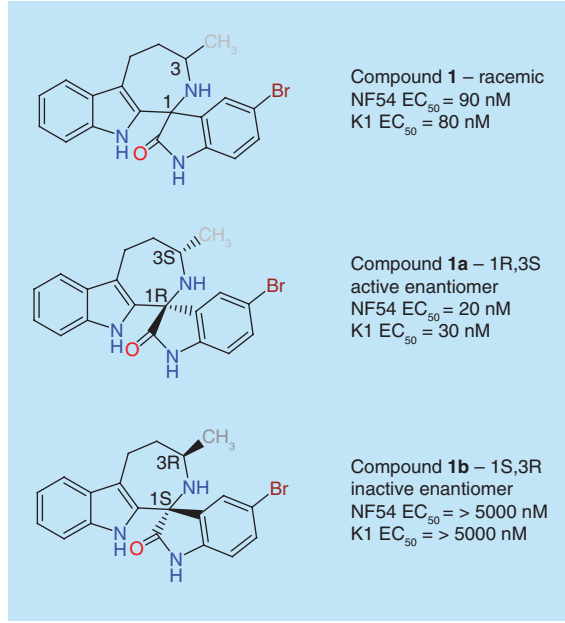

Figure 2. Molecular structure of the lead compound.
The racemic **1,** active enantiomer **1a** (1R,3S) and inactive enantiomer **1b** (1S,3R).
Data taken with permission from [9].

In a subsequent study, Yeung and coworkers made alterations to the central seven-membered azepine ring [4] (Figure 3). Adding another carbon atom to the azepine ring of compound **2** (NF54 IC_{50} = 84nM) was found to produce an inactive compound (structure not shown: NF54 IC_{50} > 5000 nM); however, potency was discovered to increase threefold after removing a carbon atom to make a 6-membered ring tetrahydro-β-carboline derivative (**4**) (Figure 3). Removal of the C3 methyl from the tetra-hydro-β-carboline structure resulted in nearly a fivefold loss of potency (**5**); however, the authors reported that its removal did not affect the potency for the azepineindole structure (**3**). The C3 methyl could only be substituted with trifluoromethyl.

The spiroindolones were identified as good drug candidates as they generally had good *in vitro* solubility and permeability, were not cytotoxic to human cell lines, had low cardiotoxicity potential, low genotoxicity and did not significantly bind to human receptors, kinases or ion channels [9]. Studies demonstrated a significant difference in the metabolic stability and CYP450 inhibition between the pairs of enantiomers, with the inactive 1S,3R having more favorable properties [9]. In light of this, Yeung and coworkers used a microsomal clearance assay to predict the metabolic stability and found that the active 1R,3S enantiomers had a high clearance, poor metabolic stability with liver microsomes and inhibited CYP2C9 preferentially (Table 1).

The benzene ring of the indole moiety was identified as being susceptible to metabolism by oxidation and therefore leading to high clearance. A systematic approach was taken to modifying the indole ring of compound **4a** to improve its half-life in the presence of liver microsomes (Figure 4). Aryl halides are usually too stable to be metabolized so the team added halides to the benzene ring to protect it from oxidation. Substituting a fluorine atom at C7 position of the indoline was discovered to be the most effective in increasing the half-life (**7a**) [4]. It was reported that substitutions on C5, C6 and C8 did not improve the metabolic stability; however, they did increase the potency with substitutions at C6 and C7 being the most effective (**9a** and **10a**).

Although the spiroindolones had been identified as potential new antimalarial drugs, their mechanism of action was as yet unknown. As compound **9a** (NITD609, Figure 5) showed the best combination of potency and oral exposure, this was taken forward for further preclinical evaluation.

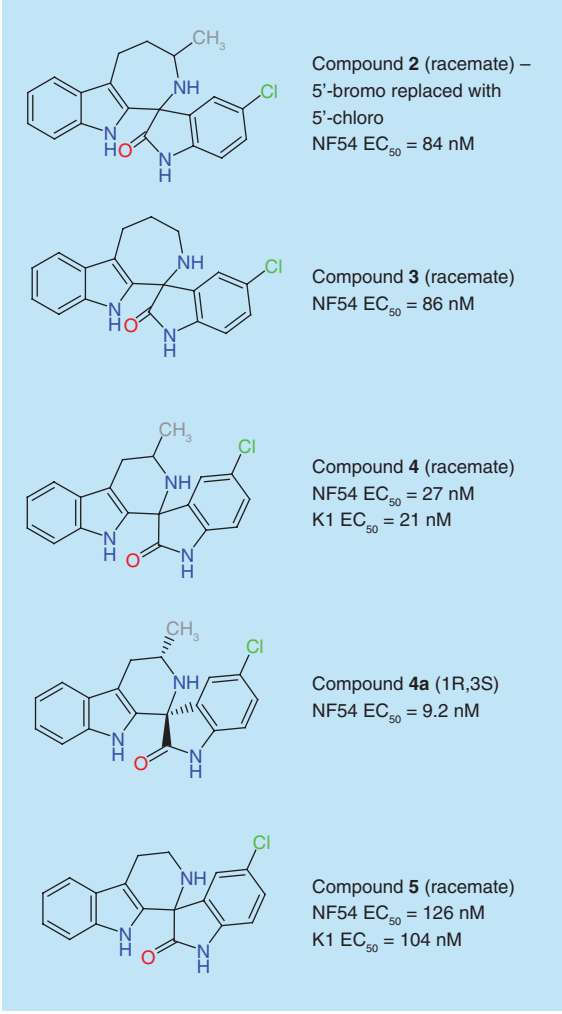

Figure 3. Compounds 2, 3, 4, 4a & 5′-bromo replaced with 5′-chloro (2). Size reduction of the azepine ring to give compound **4.** Removal of the methyl from the 7-membered ring does not affect potency (**2** & **3**); however decreases potency fivefold when removed from the 6-membered ring (**4** & **5**).
Data taken with permission from [9].

NITD609 displays antimalarial activity against the asexual blood stage, gametocyte & oocyte stages of *Plasmodium*

The optimizations from *in vitro* studies using microsomal clearance assays proved to correspond well to antimalarial activity in the *P. berghei*-infected mouse model with **4a, 9a** and **10a,** demonstrating better efficacy in reducing parasitemia than chloroquine and artesunate [4]. Each of the spiroindolones was found to prolongsurvival of the mice more than chloroquine and artesunate, when a single oral dose of 30 mg/kg was administered (Table 2). Even better results were achieved when dosed orally once daily for 3 days with 60–90% of mice being cured.

Rottmann *et al.* reported that NITD609 achieved *in vitro* inhibitory concentration (IC_{50}) values of 0.5 to 1.4 nM against a panel of wild-type and drug-resistant *P. falciparum,* with no significant decrease in activity against the drug-resistant strains [8]. Resistant strains included those with resistance against chloroquine, pyrimethamine and mefloquine. Artemisinin-resistant strains were not included in the panel, possibly as no validated *in vitro* assay to correlate susceptibility to artemisinin was available at that time [5].

The team performed *ex vivo* assays using fresh isolates of *P. falciparum* and *P. vivax* from malaria patients on the Thai-Burmese border where chloroquine resistance is known to occur [8]. NITD609 and artesunate were found to be equally effective with IC_{50} <10 nM against both *P. falciparum* and *P. vivax*. The asexual blood stages are associated with the morbidity and mortality of malaria. *In vitro* sensitivity assays using *P. falciparum* at ring, trophozoite and schizont phases of the human blood stages determined that NITD609 was most effective against schizonts [8].

As well as being effective against the asexual blood stages, a study led by Sauerwein found that NITD609 acted in a dose-dependent manner against the sexual gametocytes which are responsible for transmission of the parasite [11]. Most existing antimalarial drugs do not effect gametocytes therefore patients treated with these drugs can still transmit malaria. NITD609 was discovered to be more effective in clearing gametocytes than lumefantrine, primaquine and artemether. In this *in vitro* study the efficacy of NITD609 in clearing gametocytes could not be compared with that of primaquine, which is used in human patients to prevent transmission *in vivo* as it does not have antimalarial activity *in vitro.* The lack of *in vitro* activity of prima-

Table 1. Pharmacokinetic profile of spiroindolone 4.

Compound	4 (racemate)	4a (1R,3S)	4b (1S,3R)
NF54 IC_{50} (nM)	27	9.2	>5000
In vitro (liver microsomes), clearance CL_{int}			
– Mouse	Medium	High	Low
– Human	Medium	High	Low
In vitro (liver microsomes), microsomal half-life $t_{1/2}$(min)			
– Mouse	26.5	1.8	103
– Human	9.9	1.2	95
CYP2C9 inhibition (μM)	n/a	1.51	>10.00
In vivo (mice) clearance CL (ml/min/kg)	n/a	49.66	n/a

In vitro metabolic stability measured using liver microsomes. *In vivo* clearance measured in mice at a single 5 mg/kg iv. dose.
CL: Clearance; CLint: Intrinsic clearance; n/a: Not available.
Data taken from [4,9].

quine was expected as it is a prodrug and it is necessary for it to be metabolized to induce its gametocytocidal properties. NITD609 also was found to decrease the oocyte count when added to the blood meal of mosquitos in a standard membrane feeding assay [11].

These results showed that NITD609 not only acted on the asexual blood stages of the parasite but also on the sexual stages that are involved in transmission of malaria, however higher concentrations were required. NITD609 was found not to prevent infection of *P. berghei* mice when given prophylactically before administration of a sporozoite injection [12], indicating that NITD609 was ineffective against the liver stages of *Plasmodium*.

Spiroindolones target PfATP4

Using an incorporation assay with radiolabeled methionine and cysteine Rottmann *et al.* demonstrated that NITD609 blocked protein synthesis in *P. falciparum* within 1 h [6,8]. This effect was observed to be similar to that of the known protein translator inhibitors anisomycin and cycloheximide, but contrasted with artemisinin and mefloquine, suggesting a different mechanism of action.

Rottmann *et al.* and Flannery *et al.* used *in vitro* genetic methods to determine the likely target of NITD609 [8,13]. Malaria parasites were grown in the presence of a test compound until resistant strains developed. For NITD609 it took 3–4 months of *in vitro* selection to increase the IC_{50} seven- to ten-fold [8,13] indicating that NITD609 does not readily select for high-level resistance *in vitro*. Genomic analysis was used to compare the parent and resistant lines which enabled identification of the genes involved with the resistance. Most of the differences in the NITD609-resistant line were found in the gene for the P-type cation-transporter ATPase4 (PfATP4). This was supported by the reverse genetic approach of creating transgenic parasites with mutations on *pfatp4*, which the authors showed were resistant to the spiroindolones NITD609 and NITD678, but not artemisinin and mefloquine.

The role of membrane transport proteins in the malaria parasite

A malaria parasite that has infected a human erythrocyte needs to acquire key nutrients from the extracellular environment and export metabolites to support its high level of metabolic and biosynthetic activity, while maintaining its own cytosolic composition. The normal rate of uptake across the erythrocyte plasma membrane of some of these nutrients does not meet the requirements of the parasite and it may also be in competition with the host cell for these nutrients [14].

Human blood plasma is a high-[Na^+]/low-[K^+] environment and uninfected human erythrocytes are a low-[Na^+]/high-[K^+] environment [15]. Around 12–14 h after entering a human erythrocyte *P. falciparum* creates new permeability pathways in the plasma membrane of the host erythrocyte increasing its permeability. This enables the uptake of nutrients into the infected cell and, consequently, also allows the flow of Na^+ and K^+ across their respective concentration gradients so they reach levels close to those in the extra-erythrocytic plasma [15]. Even though this causes increased [Na^+] in its extracellular environment the parasite is able to maintain a low cytosolic [Na^+] [15,16].

Some protozoa and lower plants expel Na^+ via an exitus natrus (ENA) P-type Na^+-ATPase, which is closely related to the sarcoplasmic/endoplasmic reticulum Ca^{2+}-ATPases (SERCA) and plasma membrane Ca^{2+}-ATPases (PMCA) [15]. It was known that the

P. falciparum genome codes for 13 P-type ATPases, two of which are known to be Ca^{2+}-ATPases but none had been identified as Na^{+}-ATPase.

PfATP4 is a P-type Na^{+}-ATPase

PfATP4 belongs to a subclass (Type 4) of P-type ATPases that are unique to apicomplexan organisms [17]. P-type ATPase is a family of evolutionary related membrane-bound pumps that self-phosphorylate at a conserved aspartate residue. Most P-type ATPases pump cations enabling the maintenance of electrochemical gradients across cell membranes. The absence of PfATP4 in mammals makes it a good drug target. Until recently PfATP4 was believed to be a P-type Ca^{2+}-ATPase due to its similarity with the Ca^{2+}-ATPases of the endoplasmic reticulum [17,18], however, recent studies indicated it is in fact a P-type Na^{+}-ATPase [15,19] (discussed in more detail later in this section).

PfTP4 is a 190 kDa protein found in the parasite plasma membrane [20]. Using genetic sequencing Krishna and coworkers showed that it contained the features common to P-type ATPases, including

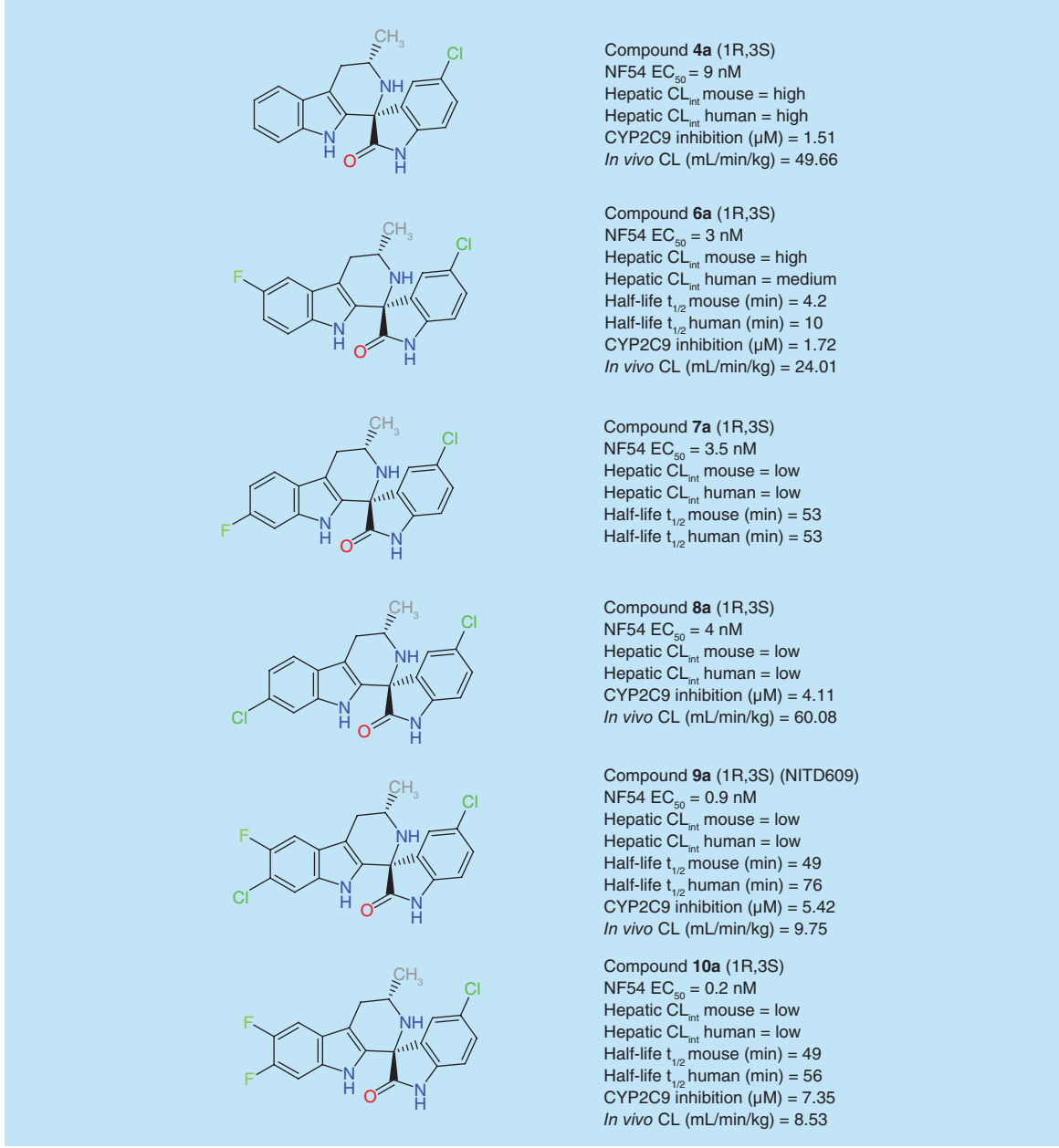

Figure 4. Substitutions on the indole ring system improved the metabolic stability and potency of the spiroindolones.
Data taken with permission from [4,9].

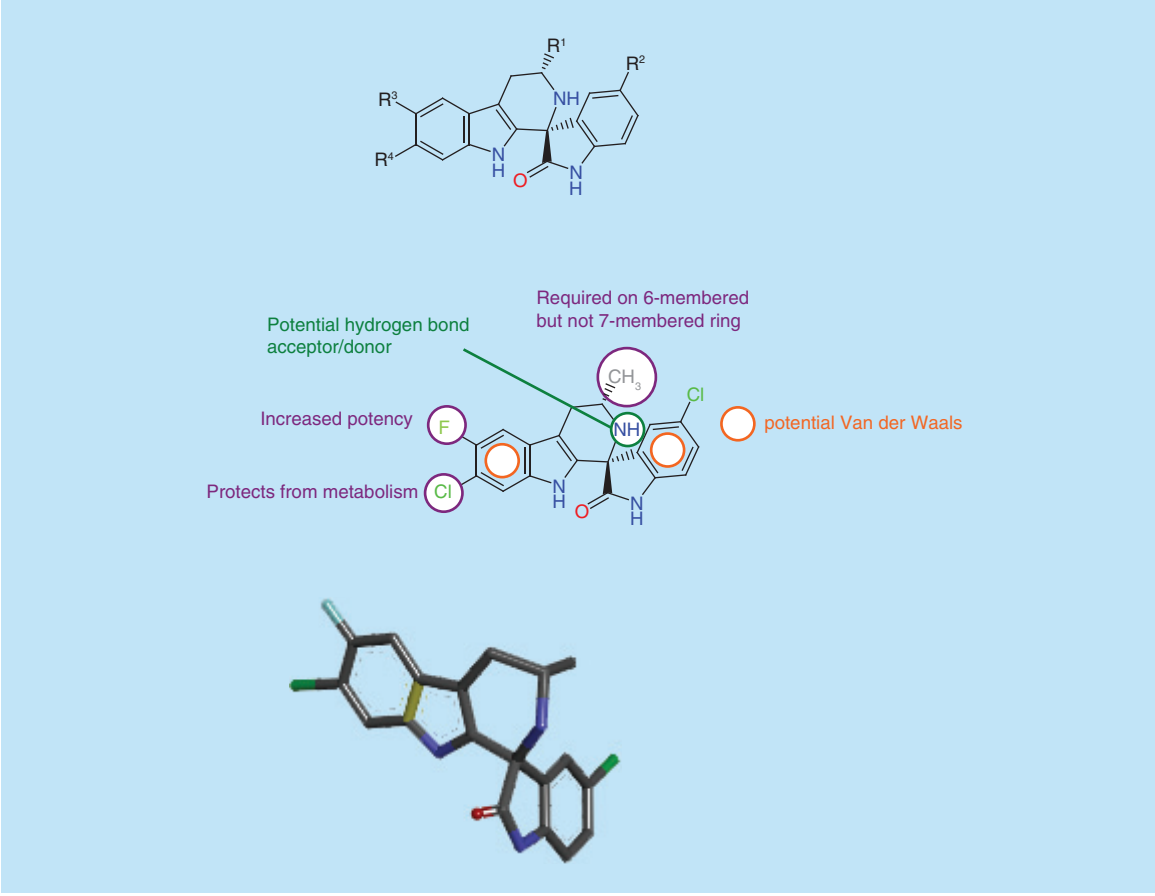

Figure 5. Top: general chemical structure of spiroindolones; middle: molecular structure of NITD609 showing key features; bottom: 3D structure of NITD609 drawn using Discovery Studio 4.5.R1 = CH3 or CF3; R2 = Cl or Fl; R3 = H, F or CL; R4 = H, F or Cl.

sequence motifs of a highly conserved phosphorylation site and nucleotide-binding site [17]. Modeling techniques revealed ten transmembrane helices and that mutations associated with spiroindolone resistance were localized in these transmembrane helices (Figure 6). The team reported that PfATP4 has an extended hydrophilic N-terminal region and lacks the long hydrophilic C-terminal seen in plasma-membrane-type ATPases. It was posited that the extended M7/M8 extracellular loop, which is has a high proportion of acidic residues, is involved in ion transport [17].

Spillman *et al.* investigated the effect of a variety of ionophores and ion transport inhibitors on Na^+ regulation in *P. falciparum* [15]. The known P-type ATPase inhibitor sodium orthovanadate was found to impair Na^+ regulation as did the known ENA Na^+-ATPase inhibitor furosemide, suggesting the involvement of ENA P-type Na^+-ATPase in maintaining the low cytosolic (Na^+), despite the high extracellular levels. Ouabain, which inhibited all known Na^+/K^+-ATPases at the concentrations used, was discovered to have no significant effect on $(Na^+)_i$ indicating that Na^+/K^+-ATPases were not involved. When the parasites were suspended in a glucose-free extracellular environment, which causes depletion of ATP, an increase in $(Na^+)_i$ was observed, which also supports the involvement of an ATPase in maintaining the low $(Na^+)_i$. Analysis of the amino acid sequence showed that PfATP4 share an amino acid sequence which is known to be highly conserved in ENA Na^+-ATPases and important for Na^+ transport. This sequence is not present in SERCA, PMCA or Na^+/K^+-ATPases.

Spillman *et al.* proposed that PfATP4 acts as an ENA Na^+-ATPase and actively pumps Na^+ out of the intra-erythrocytic parasite and that the efflux of Na^+ is associated with an influx of H^+ into the parasite (Figure 7) [15]. A further study demonstrated that the acid load caused by the influx of H^+ is likely to be countered by the extrusion of H^+ by a V-type H^+-ATPase [19].

Spiroindolones inhibit PfATP4

Spillman *et al.* demonstrated that four different spiroindolones caused an increase in $[Na^+]$ in a dose-dependent manner and the order of potency in increasing (Na^+) corresponded their ranking inhibiting parasite

proliferation [15]. Spiroindolone NITD246 was shown to reduce membrane-associated ATPase activity in membrane preparations from infected erythrocytes suspended in a high concentration of Na^+. It was also shown that PfATP4 mutations corresponding with spiroindolone resistance reduced sensitivity to Na^+ disruption and ATPase activity by spiroindolones. These results supported the hypothesis that spiroindolones inhibit PfATP4 preventing sodium ions being pumped out of the parasite and leading to a fatal disruption of parasite sodium homeostasis (Figure 7).

Determination of 3D structure required

The 3D structure of PfATP4 has been predicted using Modeling techniques; however, it has not yet been determined by x-ray crystallography. It is important that the structure of PfATP4 and its binding with ligands, including the spiroindolones and other drugs that target is ascertained. Understanding the active sites of PfATP4 and the binding interactions that occur will allow more effective drugs to be created.

Pharmacokinetics

An important factor in a successful antimalarial treatment is ensuring patient compliance which can be improved by reducing the pill burden and treatment duration. Existing antimalarial drugs have to be taken from one- to four-times daily for up to seven days [22] which is often difficult to achieve in areas where there is a lack of medical supervision.

The pharmacokinetic properties observed by Rottmann *et al.* when NITD609 was administered to mice and rats indicated that a once-daily dosing regimen might be appropriate [8]. It had excellent oral bioavailability, a good half-life, moderate volume of distribution and low systemic clearance. A further pharmacokinetic–pharmacodynamic (PK–PD) study to determine whether the antimalarial effect was concentration dependent or time dependent suggested it was time dependent, however further investigation is required [23]. PK–PD data from this study have been used to define appropriate dosing regimens.

Safety & selectivity of NITD609 *in vitro*

The safety of new antimalarial drugs is essential, particularly due to the vulnerability of the patient population, which includes many young children, pregnant women and those with comorbidities, living in areas that often have limited medical resources. The malaria parasite within the human body is the intended target for NITD609 therefore it is important that it is not cytotoxic to human cells at the concentrations required for parasite cytotoxicity. In the study by Rottmann *et al.* NITD609 showed no significant cytotoxicity against a panel of *in vitro* mammalian cell lines [8]. For each of the cell lines tested the concentration of NITD609 that led to 50% cell death (CC_{50}) was at least 10 µM. Since the IC_{50} was <1 nM the selectivity index (CC_{50}/IC_{50}) >10,000. Some antimalarial drugs can be cardiotoxic as they inhibit hERG channels; however, NITD609 showed low binding affinity to hERG as well as other human ion channels, G-protein-coupled receptors and enzymes. When administered to rats for 14 days at 10- to 20-times the calculated effective dose required to reduce parasitemia by 99% (ED_{99}) no adverse events were observed.

Clinical trials

NITD609 (which is now known as KAE609 or cipargamin) has undergone a Phase II clinical trial in three locations in Thailand to assess its antimalarial efficacy, safety and adverse events (ClinicalTrials.gov number NCT01524341) [24]. KAE609 was administered to adults with uncomplicated *P. vivax* or *P. falciparum* malaria at 30 mg per day for 3 days. The study was small with only 21 patients; however, the results were very encouraging. KAE609 cleared the parasites rapidly from the blood of the patients with median complete parasite clearance time of 12 hours. The median parasite half-life clearance was 0.95 h for *P. vivax* and 0.90 h for *P. falciparum,* which is excellent when compared with artensunate for which less than 1% of patients infected with *P. falciparum* have half-life clearance of under 1 h.

The safety, tolerability and pharmacokinetics of KAE609 in healthy male adult patients after single and multiple oral dosing was assessed in a randomized,

Table 2. *In vivo* antimalarial activity in *Plasmodium berghei*-infected mouse model.

Compound	1 × 30 mg/kg			3 × 30 mg/kg		
	Activity (%)	Survival (days)	Cure rate (%)	Activity (%)	Survival (days)	Cure rate (%)
Chloroquine	99.7	8.7	0	99.9	14.0	0
Artesunate	92.2	7.3	0	99.0	11.8	0
4a	99.9	10.7	0	99.9	18.8	60
9a (NITD609)	99.6	13.3	0	99.8	29.1	90
10a	99.6	12.0	0	99.8	23.8	80

Data taken with permission from [4].

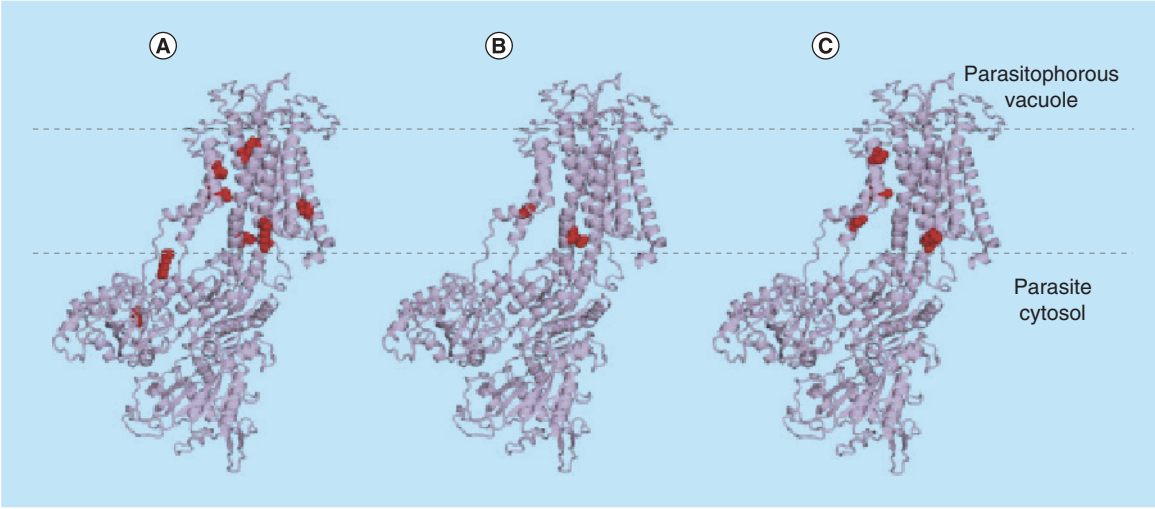

Figure 6. Homology model of PfATP4 showing residues associated with resistance. (A) Spiroindolones NIDT609 and NIDT678; **(B)** MMV007272 & MMV0011567, carboxamides from the Malaria Box; **(C)** aminopyrazole GNF-Pf4492. Amino acids associated with resistance are shown in red.
Adapted with permission from [21] © Elsevier (2015).

double-blind, placebo-controlled Phase I study [25]. KAE609 was generally well tolerated; however, some mild to moderate adverse events were recorded which were mostly gastrointestinal and genitourinary and increased with rising doses. Data from this trial [25] and the PK–PD study of Lakshminarayana *et al.* [23] led to the suggested dose of 30 mg/kg/day [21].

A Phase I clinical evaluation of the co-administration of KAE609 and piperaquine (a long-acting antimalarial used in combination with artemisinins) did not indicate adverse interactions. Piperaquine is known to increase the QT interval, however, this was not the case for KAE609 [26].

Two further Phase II clinical trials have been completed but the results not yet published [27]. One to find the minimum inhibitory concentration for a single dose of KAE609 to reduce parasitemia to zero in adult male patients with *P. falciparum* monoinfec-

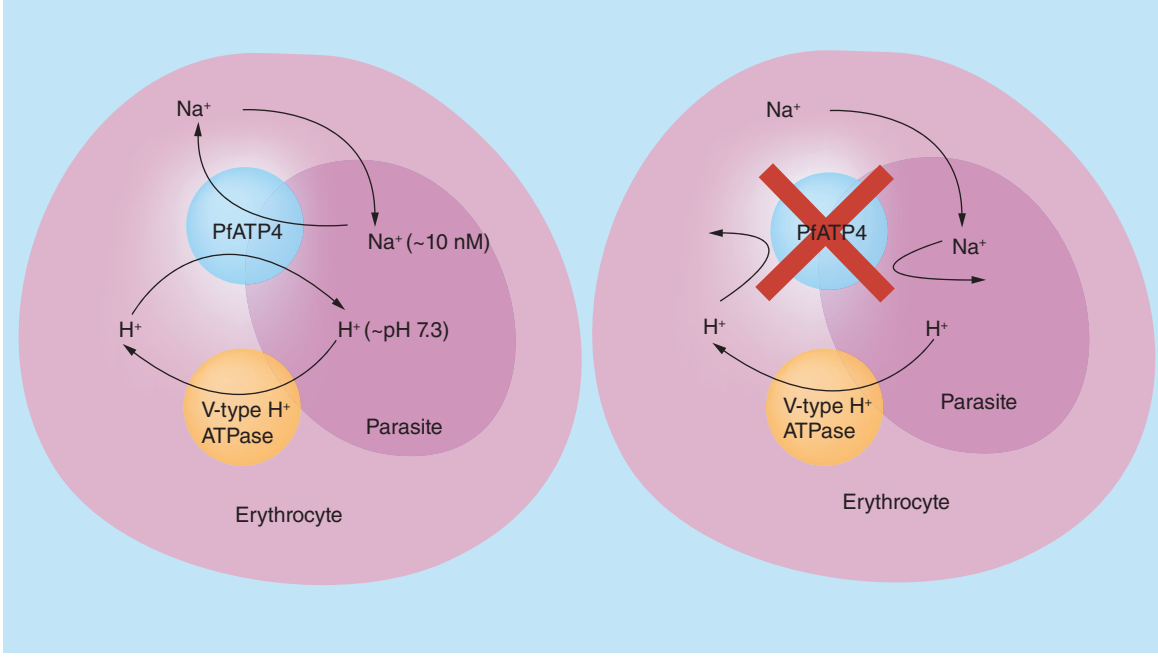

Figure 7. Proposed mechanism of action of spiroindolones targeting PfATP4 in the plasma membrane of *Plasmodium falciparum* [15,21]. Inhibition of PfATP4 by spiroindolones (indicated by red cross in the erythrocyte on right) leads to a rise in intracellular Na^+ and increase in intracellular pH.
Adapted with permission from [21] © Elsevier (2015) and from [15].

tion (ClinicalTrials.gov Identifier: NCT01836458), this will help to identify the optimal dose of KAE609. Another to assess the efficacy and safety of KAE609 in adults with acute malaria mono-infection (ClinicalTrials.gov Identifier: NCT01860989). A Phase I clinical trial to determine the effectiveness of KAE609 in reducing asexual and sexual blood-stage *P. falciparum* infection and preventing transmission to mosquitos is expected to complete in February 2016 (ClinicalTrials.gov Identifier: NCT02543086).

PfATP4 pathway targeted by diverse structures

In a recent *in vitro* study by Lehane *et al.*, 28 out of 400 (7%) compounds in the 'Malaria Box' were found to affect Na^+ and pH regulation in a manner consistent with PfATP4 inhibition [28]. Six of these, which had chemically diverse structures, were analyzed further and were all discovered to have reduced efficacy against spiroindolone-resistant parasites with pfatp4 mutations, indicating that they all interact with PfATP4. Flannery *et al.* showed that aminopyrazoles also target PfATP4 and showed cross resistance with spiroindolones [29]. Aminopyrazoles have a different structure to spiroindolones; however, resistance to both classes of compound is conferred by mutations in the transmembrane region of PfATP4 [29]. Characteristics of the resistance led Flannery *et al.* to suggest that the binding sites of spiroindolones and aminopyrazoles overlap [29]. These results suggest that PfATP4 is important for parasite survival, can be inhibited by a variety of compounds and is readily accessed by compounds in the extracellular medium. Researchers at GlaxoSmithKline have identified at least four further scaffolds unrelated to NITD609 that may act via the same PfATP4 pathway [30]. These results indicate that PfATP4 may be an important target in the fight against malaria and certainly warrants further research to understand its action, molecular structure and binding sites.

Repurposing of NITD609 for use against other apicomplexan parasites

As well as its activity against *Plasmodium,* NITD609 is also active against the related apicomplexan parasite *Toxoplasma gondii* which causes toxoplasmosis [31]. *Toxoplasma gondii* ATPase4 (TgATP4), which corresponds to PfATP4, was identified as the likely target. Modeling techniques showed that PfATP4 and TgATP4 share a large degree of sequence identity particularly around the transmembrane region of the ATPase4 structure where the spiroindolone binding site is proposed to be and the residues involved in drug resistance.

Future perspective

NITD609 is currently in Phase II clinical trials and is the first antimalarial drug with a novel action to reach this stage since atovaquone/proguanil in 1996 [6]. To reduce the risk of resistance developing antimalarial drugs should always be administered in combination therefore if it is successful in clinical trials a suitable partner drug will need to be identified which could delay its introduction into clinical use. Novartis anticipates submitting KAE609 for approval in 2017 pending the favorable results of ongoing clinical trials [32]. The chiral centers of the spiroindolones may cause

Executive summary

- Resistance of *Plasmodium* to artemisinin emphasizes the need for new antimalarial drugs with a novel mode of action.
- Spiroindolones were discovered to have antimalarial activity using whole-cell screening methods, however, their target and mode of action were unknown.
- It was determined that the 1R,3S configuration was required for activity against *Plasmodium*.
- Optimization of the spiroindolone using structure–activity relationship analysis lead improved both potency and pharmacokinetics and led to drug candidate NIT609.
- Spiroindolones inhibit PfATP4 of the *Plasmodium* parasite resulting in a fatal increase in sodium ions in the parasite.
- PfATP4 is a P-type Na^+-ATPase located in the parasite plasma membrane that pumps sodium ions out of the parasite.
- The spiroindolones have a distinct mechanism of action from the existing antimalarial drugs.
- *In vitro* spiroindolones do not readily select for resistance and do not show cross-resistance to existing antimalarial drugs.
- Pharmacokinetic studies indicate NITD609 may be compatible with once-daily oral dosing.
- NITD609 is currently in Phase II clinical trials where so far it has shown encouraging results.
- The crystal structure of PfATP4 and its binding interactions with the spiroindolones or other drugs has not been determined.
- Other compounds in the Malaria Box, with diverse molecular structures, also appear to target PfATP4. This suggests that PfATP4 is an important target that should be investigated further.

them to have a high production cost [9,29], therefore exploration of alternative PfATP4 inhibitors may lead to cheaper options.

PfATP4 is emerging as an important target in the fight against malaria and further research is needed to understand its structure, function and how drugs may target it in the fight against malaria. The 3D, crystal structure of the PfATP4 protein should be determined as well as its binding interactions with the spiroindolones and some of the diverse compounds from the Malaria Box. With this knowledge a rational approach can be utilized to create further drugs for the treatment of malaria and possibly other apicomplexan parasites such as *Toxoplasma gondii*.

References

Papers of special note have been highlighted as:
• of interest; •• of considerable interest

1 Wells TNC, Alonso PL, Gutteridge WE. New medicines to improve control and contribute to the eradication of malaria. *Nat. Rev. Drug Discov.* 8(11), 879–891 (2009).

2 World Health Organisation. World Malaria Report 2014. www.who.int/malaria/publications/world_malaria

3 Greenwood B. Treatment of malaria – a continuing challenge. *N. Engl. J. Med.* 371(5), 474–475 (2014).

4 Smith PW, Diagana TT, Yeung BKS. Progressing the global antimalarial portfolio: finding drugs which target multiple Plasmodium life stages. *Parasitology* 141(1), 66–76 (2014).

5 Wongsrichanalai C, Sibley CH. Fighting drug-resistant *Plasmodium falciparum*: the challenge of artemisinin resistance. *Clin. Microbiol. Infect.* 19(10), 908–916 (2013).

6 Mäser P, Wittlin S, Rottmann M, Wenzler T, Kaiser M, Brun R. Antiparasitic agents: new drugs on the horizon. *Curr. Opin. Pharmacol.* 12(5), 562–566 (2012).

7 Wells TNC. Is the tide turning for new malaria medicines? *Science* 329(5996), 1153–1154 (2010).

8 Rottmann M, McNamara C, Yeung BKS *et al.* Spiroindolones, a potent compound class for the treatment of malaria. *Science* 329(5996), 1175–1180 (2010).

•• **Discovery and characterization of NIDT609 as a potent antimalarial drug candidate.**

9 Yeung BKS, Zou B, Rottmann M *et al.* Spirotetrahydro beta-carbolines (spiroindolones): a new class of potent and orally efficacious compounds for the treatment of malaria. *J. Med. Chem.* 53(14), 5155–5164 (2010).

10 Centers for Disease Control and Prevention. Malaria Biology (2012). www.cdc.gov/malaria/about/biology/

11 van Pelt-Koops JC, Pett HE, Graumans W *et al.* The spiroindolone drug candidate NITD609 potently inhibits gametocytogenesis and blocks *Plasmodium falciparum* transmission to anopheles mosquito vector. *Antimicrob. Agents Chemother.* 56(7), 3544–3548 (2012).

12 Meister S, Plouffe DM, Kuhen KL *et al.* Imaging of Plasmodium liver stages to drive next-generation antimalarial drug discovery. *Science* 334(6061), 1372–1377 (2011).

13 Flannery EL, Fidock DA, Winzeler EA. Using genetic methods to define the targets of compounds with antimalarial activity. *J. Med. Chem.* 56(20), 7761–7771 (2013).

14 Kirk K, Lehane AM. Membrane transport in the malaria parasite and its host erythrocyte. *Biochem. J.* 457(1), 1–18 (2014).

15 Spillman NJ, Allen RJW, McNamara CW *et al.* Na(+) regulation in the malaria parasite Plasmodium falciparum involves the cation ATPase PfATP4 and is a target of the spiroindolone antimalarials. *Cell Host Microbe* 13(2), 227–237 (2013).

•• **Proposes mechanism for PfATP4 regulating Na^+ in Plasmodium and how spiroindolones disrupt Na^+ homeostasis.**

16 Mauritz JMA, Seear R, Esposito A *et al.* X-ray microanalysis investigation of the changes in Na, K, and hemoglobin concentration in plasmodium falciparum-infected red blood cells. *Biophys. J.* 100(6), 1438–1445 (2011).

17 Krishna S, Woodrow C, Webb R *et al.* Expression and functional characterization of a *Plasmodium falciparum* $Ca2^+$-ATPase (PfATP4) belonging to a subclass unique to apicomplexan organisms. *J. Biol. Chem.* 276(14), 10782–10787 (2001).

18 Dyer M, Jackson M, McWhinney C, Zhao G, Mikkelsen R. Analysis of a cation-transporting ATPase of Plasmodium falciparum. *Mol. Biochem. Parasitol.* 78(1–2), 1–12 (1996).

19 Spillman NJ, Allen RJW, Kirk K. Na+ extrusion imposes an acid load on the intraerythrocytic malaria parasite. *Mol. Biochem. Parasitol.* 189(1–2), 1–4 (2013).

20 Krishna S, Webb R, Woodrow C. Transport proteins of Plasmodium falciparum: defining the limits of metabolism. *Int. J. Parasitol.* 31(12), 1331–1342 (2001).

21 Spillman NJ, Kirk K. The malaria parasite cation ATPase PfATP4 and its role in the mechanism of action of a new arsenal of antimalarial drugs. *Int. J. Parasitol. Drugs Drug Resist.* 5(3), 149–162 (2015).

Acknowledgements

The author would like to thank her tutor G Patrick, Y Xu and S Pitman for their guidance.

Financial & competing interests disclosure

An earlier version of the manuscript was a part of the course work for the Master module: Medicinal Chemistry at The Open University (S807 Molecules in Medicine). The author has no other relevant affiliations or financial involvement with any organization or entity with a financial interest in or financial conflict with the subject matter or materials discussed in the manuscript apart from those disclosed.

No writing assistance was utilized in the production of this manuscript.

22 Dandapani S, Comer E, Duvall JR, Munoz B. Hits, leads and drugs against malaria through diversity-oriented synthesis. *Future Med. Chem.* 4(18), 2279–2294 (2012).

23 Lakshminarayana SB, Freymond C, Fischli C *et al.* Pharmacokinetic–pharmacodynamic analysis of spiroindolone analogs and KAE609 in a murine malaria model. *Antimicrob. Agents Chemother.* 59(2), 1200–1210 (2015).

- **Investigates the relationship between dose and efficacy of spiroindolones to identify PK–PD relationship useful in further drug design and optimization.**

24 White NJ, Pukrittayakamee S, Phyo AP *et al.* Spiroindolone KAE609 for Falciparum and Vivax Malaria. *N. Engl. J. Med.* 371(5), 403–410 (2014).

25 Leong FJ, Li R, Jain JP *et al.* A first-in-human randomized, double-blind, placebo-controlled, single- and multiple-ascending oral dose study of novel antimalarial spiroindolone KAE609 (Cipargamin) to assess its safety, tolerability, and pharmacokinetics in healthy adult volunteers. *Antimicrob. Agents Chemother.* 58(10), 6209–6214 (2014).

26 Stein DS, Jain J, Lickliter J *et al.* A Phase 1 evaluation of the pharmacokinetic/pharmacodynamic interaction of the antimalarial agents KAE609 and piperaquine (PPQ). *Malar. J.* 13(Suppl. 1), P85 (2014).

27 ClinicalTrials search: KAE609. https://clinicaltrials.gov/ct2/results

28 Lehane AM, Ridgway MC, Baker E, Kirk K. Diverse chemotypes disrupt ion homeostasis in the malaria parasite. *Mol. Microbiol.* 94(2), 327–339 (2014).

29 Flannery EL, McNamara CW, Kim SW *et al.* Mutations in the P-Type cation-transporter ATPase 4, PfATP4, mediate resistance to both aminopyrazole and spiroindolone antimalarials. *ACS Chem. Biol.* 10(2), 413–420 (2015).

30 Gamo F-J. Antimalarial drug resistance: new treatments options for Plasmodium. *Drug Discov. Today Technol.* 11, 81–88 (2014).

31 Zhou Y, Fomovska A, Muench S, Lai B-S, Mui E, McLeod R. Spiroindolone that inhibits PfATPase4 is a potent, cidal inhibitor of *Toxoplasma gondii* tachyzoites *in vitro* and *in vivo*. *Antimicrob. Agents Chemother.* 58(3), 1789–1792 (2014).

32 Cully M. Trial watch: next-generation antimalarial from phenotypic screen shows clinical promise. *Nat. Rev. Drug Discov.* 13(10), 717 (2014).

Editorial

For reprint orders, please contact reprints@future-science.com

Future Medicinal Chemistry

Loading antimalarial drugs into noninfected red blood cells: an undesirable roommate for *Plasmodium*

"...most antimalarials start affecting the infected cell relatively late in the intraerythrocytic parasite life cycle, when their effect is probably often too short to be lethal to *Plasmodium*."

Keywords: malaria • nanomedicine • *Plasmodium* • red blood cell • targeted drug delivery

Ernest Moles
Nanomalaria Unit, Institute for Bioengineering of Catalonia (IBEC), Baldiri Reixac 10–12, Barcelona ES-08028, Spain
and
Barcelona Institute for Global Health (ISGlobal, Barcelona Ctr. Int. Health Res. [CRESIB], Hospital Clínic-Universitat de Barcelona), Rosselló 149–153, Barcelona ES-08036, Spain
and
Nanoscience & Nanotechnology Institute (IN²UB), University of Barcelona, Martí i Franquès 1, Barcelona ES-08028, Spain

Xavier Fernàndez-Busquets
Author for correspondence:
Nanomalaria Unit, Institute for Bioengineering of Catalonia (IBEC), Baldiri Reixac 10–12, Barcelona ES- 8028, Spain
and
Barcelona Institute for Global Health (ISGlobal, Barcelona Ctr. Int. Health Res. [CRESIB], Hospital Clínic-Universitat de Barcelona), Rosselló 149–153, Barcelona ES-08036, Spain
and
Nanoscience & Nanotechnology Institute (IN²UB), University of Barcelona, Martí i Franquès 1, Barcelona ES-08028, Spain
xfernandez_busquets@ub.edu

The malaria parasite, *Plasmodium* spp., is a delicate unicellular organism unable to survive in free form for more than a couple of minutes in the bloodstream. Upon injection in a human by its *Anopheles* mosquito vector, *Plasmodium* sporozoites pass through the liver with the aim of invading hepatocytes. Those which succeed spend inside their host cell a recovery time before replicating and entering the blood circulation as fragile merozoites, although their exposure to host defenses is extraordinarily short. Quick invasion of red blood cells (RBCs) in a process lasting just a few minutes allows the parasite to escape immune system surveillance. For most of its erythrocytic cycle the pathogen feeds mainly on hemoglobin as it progresses from the early blood stages, termed rings, to the late forms trophozoites and schizonts. Early stages are ideal targets for antimalarial therapies because drugs delivered to them would have a longer time to kill the parasite before it completes its development. However, only 6 h after invasion does the permeability of the infected erythrocyte to anions and small nonelectrolytes, including some drugs, start to increase as the parasite matures [1]. During this maturation process the parasite hydrolyzes hemoglobin in a digestive vacuole, which is the target of many amphiphilic drugs that freely cross the RBC membrane and accumulate intracellularly. As a result, most antimalarials start affecting the infected cell relatively late in the intraerythrocytic parasite life cycle, when their effect is probably often too short to be lethal to *Plasmodium*.

Malaria-infected erythrocytes: an elusive target

Several strategies to improve the activity of antimalarial drugs concern their encapsulation in nanocarriers targeted to parasitized RBCs (pRBCs), an approach that requires the existence of specific pRBC markers. 200-nm liposomes studded with heparin or antibodies raised against pRBCs have been shown to bind late forms with high selectivity [2,3], improving the activity of encapsulated antimalarial drugs up to tenfold [2,4]. In addition to the inconvenient late-stage targeting, such liposomal delivery models will also have to overcome the obstacle of timing nanocarrier administration to the precise moment of the parasite's life cycle when trophozoites and schizonts are present. The relatively short blood half-life of liposomes (in the best cases, <10 h for polyethylene glycol-coated stealth liposomes) guarantees that if injected at the wrong moment (too soon or too late), they will not last the 48 h needed to ensure that they are present for the pathogen's next cycle. In another display of cunningness, *Plasmodium* leaves virtually no external signal on the parasitized cell, and only after spending half its life inside the erythrocyte does the parasite export a significant number of receptors and transporters to the host cell plasma membrane. Most of these externally recognizable clues are present in the parasite genome as multiple variants that can be clonally expressed [5], which further complicates delivery approaches designed to specifically target pRBCs. A receptor-independent alternative for the nanovector-mediated delivery of antimalarial drugs to *Plasmodium* blood

FUTURE SCIENCE part of fsg

stages can be provided by the tubulovesicular network induced in the host cell by the pathogen during its intraerythrocytic growth, which confers pRBC accessibility to a wide range of particles up to diameters of 70 nm [6]. Indeed, polymeric nanovectors were observed to penetrate trophozoites and schizonts [7,8], possibly in a significant fraction through the tubulovesicular network, although entry of nanoparticles into early ring stages has not been unambiguously observed so far.

Is there an ideal carrier for blood-circulating drugs?

Antimalarial drug carriers should provide optimal compound half-lives in circulation, adequate clearance mechanisms, restriction of unintended drug effects in non-target cells, specific delivery to the correct tissue, and a timely initiation and termination of the therapeutic action. Considering the need to target intraerythrocytic *Plasmodium* as early in its life cycle as possible and the lack of strategies currently out there for shuttling drugs into pRBCs, it is imperative that these issues are addressed and that alternative approaches are explored. A solution to the aforementioned problems in the design of pRBC-targeted nanocarriers can perhaps be provided by one of the most adequate vascular carriers, RBCs themselves [9]. Human erythrocytes have a life span in the blood of up to 120 days, which makes them attractive carriers for intravascular delivery because they prolong drug circulation. In addition, their large size (approximately 7 μm across and around 2 μm thick) significantly restricts unintended extravasation and in principle allows for a much larger encapsulation capacity than liposomes. Other interesting features of RBCs as drug carriers are their biocompatibility and the existence of natural mechanisms for their safe elimination from the body. Actually, delivery of antimalarials to noninfected RBCs has been previously carried out in chemotherapeutic investigations, in order to examine the effects on later invading parasites. In one such study, RBCs were pretreated with the drugs halofantrine, lumefantrine, piperaquine, amodiaquine and mefloquine, which were observed to diffuse into and remain within the erythrocyte, inhibiting downstream growth of *Plasmodium* [10]. However, it should be noted that the loading of drugs into noninfected RBCs has not yet been explored in detail as a clinically feasible therapeutic strategy against malaria, in part because of a number of restrictions that must be taken into consideration.

Which are the limitations of erythrocytes as drug carriers?

A significant limiting factor for the use of RBCs as antimalarial carriers is that when present at therapeutically active concentration, the drug has to be innocuous for the cell physiology, which might not be an unsurmountable obstacle given the reduced metabolic activity of eryrthrocytes. However, loading of some antimalarial drugs like clotrimazole had been observed to predispose RBCs to oxidative damage [11], an undesirable scenario because oxidized RBCs are rapidly taken up by hepatic reticuloendothelial system macrophages. Another obstacle for the incorporation of antimalarial drugs into RBCs is drug loading itself, since most currently available protocols use a harsh *ex vivo* isolation of erythrocytes followed by drug loading through diffusion [9]. In a clinical setting, perhaps RBC-targeted immunoliposomes can come to rescue, although the incapacity of mature erythrocytes to endocyte [12] calls for the development of specific targeted drug delivery strategies independent from the receptor-mediated endocytic pathway. Moreover, the physicochemical properties of each particular antimalarial drug will constrain the nanovector composition and the corresponding drug delivery mechanism. As an example, the optimal approach for delivery of membrane-impermeable hydrophilic drugs such as fosmidomycin would be immunoliposomal fusion with the RBC membrane, which requires the incorporation of special fusogenic agents into highly fluid vesicles. Including negatively charged phospholipids in the liposome formulation has been found to be crucial for the delivery of trehalose into RBCs *in vitro* [13], but nanovector fusion can be inhibited by components found in plasma [14], and charged vesicles are quickly complexed by serum proteins that target them for clearance from circulation [15]. A possible solution consists of incorporating stealth agents onto the nanovector surface like polyethylene glycol chains or gangliosides, which neutralize vesicle charge and significantly reduce unspecific interaction events, although they can also interfere with fusion if excessive amounts are used.

> "...the loading of drugs into noninfected red blood cells has not yet been explored in detail as a clinically feasible therapeutic strategy against malaria..."

The capacity of amphiphilic antimalarial drugs (which comprise the extensive aminoquinoline and artemisinin drug derivative families) to easily cross lipid bilayers demands a careful design of their targeting liposomes. Active loading techniques based on pH gradients across liposome membranes [16] are required to efficiently encapsulate the fully ionized species of amphiphilic drugs, in combination with a saturated lipid-enriched bilayer capable of maintaining a proton gradient. As a consequence of the reduced fluidity of the resulting membrane, fusion events with targeted

cells are significantly inhibited; sustained drug delivery while the liposome is docked onto the RBC is the most likely mechanism through which such nanovectors operate. This process would be mediated by a depletion of the liposomal proton gradient by means of temperature, liposome–cell interaction events [17] and lipid transference to plasma components [18], and might be highly effective for the delivery of weak basic drugs such as those from the aminoquinoline family. These compounds, positively charged at neutral pH, will theoretically accumulate inside the cell and become entrapped by virtue of the electrochemical gradient created by the phospholipid asymmetry in RBC membranes [19], which maintains a negatively charged intracellular membrane lining. Liposomal nanovectors are also efficient carriers for hydrophobic drugs like lumefantrine and halofantrine, which can be delivered to RBCs following a sustained release process by an exchange mechanism of hydrophobic material between the apposed membranes of liposome and erythrocyte [20]. Since the liposomes adsorbed on RBC surfaces would probably sufficiently modify cell shape to target it for removal through spleen filtration, a compromise between stable drug containment and lipid bilayer fusion will have to be reached through the adequate liposome formulation, with the objective of achieving liposome–RBC merging before spleen removal while avoiding rapid drug leaking from liposomes.

It is reasonable to predict that the nanovector design limitations exposed above can be satisfactorily dealt with, and that some of the future antimalarials yet to be discovered will be harmless for erythrocytes, thus allowing for the loading in these cells of drug amounts that are lethal for *Plasmodium*. If so, the pathogen might encounter its enemy at home, right at the very moment of entering the host cell, which would have devastating effects for the parasite and significantly compromise its survival capacity. Such a strategy could be likely developed into a prophylactic treatment against erythrocyte infection.

Financial & competing interests disclosure

This work was supported by grants BIO2011–25039 and BIO2014-52872-R from the Ministerio de Economía y Competitividad, Spain, which included FEDER funds, 2014-SGR-938 from the Generalitat de Catalunya, Spain, and 2013–0584 from the FondSazione Cariplo, Italy. The authors have no other relevant affiliations or financial involvement with any organization or entity with a financial interest in or financial conflict with the subject matter or materials discussed in the manuscript apart from those disclosed.

No writing assistance was utilized in the production of this manuscript.

References

1 Kirk K. Membrane transport in the malaria-infected erythrocyte. *Physiol. Rev.* 81(2), 495–537 (2001).

2 Marques J, Moles E, Urbán P *et al.* Application of heparin as a dual agent with antimalarial and liposome targeting activities towards *Plasmodium*-infected red blood cells. *Nanomedicine* 10, 1719–1728 (2014).

3 Urbán P, Estelrich J, Cortés A, Fernàndez-Busquets X. A nanovector with complete discrimination for targeted delivery to *Plasmodium falciparum*-infected versus non-infected red blood cells *in vitro*. *J. Control. Release* 151(2), 202–211 (2011).

4 Urbán P, Estelrich J, Adeva A, Cortés A, Fernàndez-Busquets X. Study of the efficacy of antimalarial drugs delivered inside targeted immunoliposomal nanovectors. *Nanoscale Res. Lett.* 6, 620 (2011).

5 Kyes S, Horrocks P, Newbold C. Antigenic variation at the infected red cell surface in malaria. *Ann. Rev. Microbiol.* 55, 673–707 (2001).

6 Goodyer ID, Pouvelle B, Schneider TG, Trelka DP, Taraschi TF. Characterization of macromolecular transport pathways in malaria-infected erythrocytes. *Mol. Biochem. Parasitol.* 87(1), 13–28 (1997).

7 Movellan J, Urbán P, Moles E *et al.* Amphiphilic dendritic derivatives as nanocarriers for the targeted delivery of antimalarial drugs. *Biomaterials* 35(27), 7940–7950 (2014).

8 Urbán P, Valle-Delgado JJ, Mauro N *et al.* Use of poly(amidoamine) drug conjugates for the delivery of antimalarials to *Plasmodium*. *J. Control. Release* 177, 84–95 (2014).

9 Muzykantov VR. Drug delivery by red blood cells: vascular carriers designed by Mother Nature. *Expert Opin. Drug Deliv.* 7(4), 403–427 (2010).

10 Wilson DW, Langer C, Goodman CD, McFadden GI, Beeson JG. Defining the timing of action of antimalarial drugs against *Plasmodium falciparum*. *Antimicrob. Agents Chemother.* 57(3), 1455–1467 (2013).

11 Lisovskaya IL, Shcherbachenko IM, Volkova RI, Ataullakhanov FI. Clotrimazole enhances lysis of human erythrocytes induced by t-BHP. *Chem. Biol. Interact.* 180(3), 433–439 (2009).

12 Harmening DM. The red blood cell. Structure and function. In: *Clinical Hematology and Fundamentals of Hemostasis. 3rd Edition.* F. A. Davis Company, Philadelphia, PA, USA, 54–70 (1996).

13 Holovati JL, Gyongyossy-Issa MIC, Acker JP. Effect of liposome charge and composition on the delivery of trehalose into red blood cells. *Cell Preserv. Tech.* 6(3), 207–218 (2008).

14 Pires P, Simões S, Nir S, Gaspar R, Düzgünes N, Pedroso de Lima MC. Interaction of cationic liposomes and their DNA complexes with monocytic leukemia cells. *Biochim. Biophys. Acta* 1418(1), 71–84 (1999).

15 Maurer N, Fenske DB, Cullis PR. Developments in liposomal drug delivery systems. *Expert Opin. Biol. Ther.* 1(6), 923–947 (2001).

16 Madden TD, Harrigan PR, Tai LCL *et al.* The accumulation of drugs within large unilamellar vesicles exhibiting a proton gradient: a survey. *Chem. Phys. Lipids* 53(1), 37–46 (1990).

17 Kercret H, Chiovetti J, Fountain MW, Segrest JP. Plasma membrane-mediated leakage of liposomes induced by interaction with murine thymocytic leukemia cells. *Biochim. Biophys. Acta* 733(1), 65–74 (1983).

18 Scherphof G, Roerdink F, Waite M, Parks J. Disintegration of phosphatidylcholine liposomes in plasma as a result of interaction with high-density lipoproteins. *Biochim. Biophys. Acta* 542(2), 296–307 (1978).

19 Virtanen JA, Cheng KH, Somerharju P. Phospholipid composition of the mammalian red cell membrane can be rationalized by a superlattice model. *Proc. Natl. Acad. Sci. USA* 95(9), 4964–4969 (1998).

20 Fahr A, Hoogevest Pv, May S, Bergstrand N, Leigh S. Transfer of lipophilic drugs between liposomal membranes and biological interfaces: Consequences for drug delivery. *Eur. J. Pharm. Sci.* 26(3–4), 251–265 (2005).